004802

PROPERTY FILE

GEOLOGY OF THE HARPER CREEK COPPER DESPOSIT

~~082M009~~ 082M012

by

Gary David Belik

082M012

U. B. C.
GEOLOGY LIBRARY

GEOLOGY OF THE HARPER CREEK COPPER DEPOSIT

by

Gary David Belik

B.Sc., (Honors), University of British Columbia, 1970

A THESIS SUBMITTED IN PARTIAL FULFILMENT OF

THE REQUIREMENTS FOR THE DEGREE OF

MASTER OF SCIENCE

in the Department

of

Geological Sciences

We accept this thesis as conforming to the
required standard

.....

.....

.....

THE UNIVERSITY OF BRITISH COLUMBIA

November, 1973

ABSTRACT

This study investigates the geological setting of the Harper Creek copper deposit. The relation of the deposit to structure and stratigraphy as well as the age and nature of the mineralization are discussed.

Copper mineralization is confined to tabular-shaped zones within metasedimentary and metavolcanic rocks of the Eagle Bay Formation. Although mineralization does not appear to be stratigraphically controlled, stratigraphy was important for the locallization of higher-grade material. Large-scale structures appear to have had an important role in the channeling of 'ore-forming' fluids.

The deposit is thought to be genetically related to the formation of a large east-west oriented antiform. Mineralizing fluids of probable hydrothermal metamorphic origin migrated into this structure and replaced favorable host rocks. Although tenuous, evidence presented suggests the age of mineralization is between Upper Triassic (Karnian or Lower Norian) and Lower Jurassic-Upper Triassic.

CONTENTS

Page

Chapter I INTRODUCTION. 1

Location and Accessibility. 1

General Character of the Area 1

History of Development. 3

Chapter II REGIONAL GEOLOGY. 4

Rocks of Uncertain Age. 4

Monashee Group. 4

Eagle Bay Formation 4

Serpentinite. 6

Proterozoic or Paleozoic. 7

Kaza or Cariboo Group 7

Paleozoic 7

Fennell Formation 7

Cache Creek Group 7

Mesozoic. 8

Cenozoic. 8

Kamloops Group. 8

Chu Chua Formation 8

Skull Hill Formation 9

Miocene to Pliocene Plateau Basalt. 9

Tertiary? and Quaternary Volcanism. 9

Batholithic and Related Rocks 9

Chapter III PETROLOGY 11

Eagle Bay Formation 11

Unit 1. 13

Page

Unit 2. 14

Unit 3. 16

Unit 4. 16

Unit 5. 17

Unit 6. 17

Unit 6a. 18

Unit 6b. 18

Unit 7. 18

Unit 8. 19

Metamorphism of Units 1 to 8. 20

Titanium. 20

Age and Distribution of the Eagle Bay Formation . . 22

Andesite Dykes (Unit 9) 22

Chlorite-Biotite Gneiss (Unit 10) 23

Metamorphism of Unit 10 24

Chapter IV STRUCTURE 30

Eagle Bay Formation 30

Small-Scale Structures. 30

Foliations 30

Linear Structures. 33

Folds. 35

Fractures. 37

Large-Scale Structures. 38

Andesite Dykes. 38

Chlorite-Biotite Gneiss 40

Interpretation. 40

Ages of Deformation 42

Page

Chapter V MINERAL DEPOSITS 48

Mineralization 49

Main Period. 49

Sulphides 49

Stage I. 51

Stage II 53

Silicates, Oxides and Carbonates. 54

Alteration. 55

Paragenesis 56

Form of the Deposits. 58

Structural Controls. 58

Stratigraphic Controls 59

Second Period. 62

Sulphur Isotopes 62

Genesis. 63

Chapter VI POTASSIUM-ARGON AGE DETERMINATIONS 70

Chapter VII CONCLUSIONS. 72

REFERENCES 74

APPENDIX A. Description of Mineral Deposits Within Part of the Adams Lake and Bonaparte Lake Map-Areas. 77

APPENDIX B. Description of Samples used for Potassium-Argon Age Determinations 86

LIST OF TABLES

			Page
Table	I	Modal Range of Harper Creek Rocks	12
	II	General Lithologies of the Eagle Bay Formation, Harper Creek	13
	III	Titanium Values of Some Eagle Bay Rocks, Harper Creek . .	21
	IV	Structural Features of the Eagle Bay Formation, Harper Creek	41
	V	Primary and Secondary Minerals in the Harper Creek Area .	48
	VI	Sulphides Deposited During the Main Period of Mineralization, Harper Creek.	50
	VII	Potassium-Argon Age Determinations.	70

LIST OF FIGURES

			Page
Figure	1	Location map	2
	2	Geology and mineral deposits of part of the Adams Lake and Bonaparte Lake map-areas	5
	3	Plot of modal data for Thuya, Raft and Baldy batholiths	10
	4	Geology of the Harper Creek area	in pocket
	5	Schematic diagram to illustrate structures in rocks of the Eagle Bay Formation	31
	6	Plot of poles to S_2	32
	7	Plot of northwest-and northeast-plunging wrinkle lineations and average great circle for S_2	34
	8	Plot of early and late (kink and open) fold axes and average great circle for S_2	36
	9	Plot of poles to fractures	38
	10	Simplified sketch of the Raft, Thuya and Baldy batholiths	44
	11	Sequence of deposition of primary minerals during the main period of mineralization.	57
	12	Structure Contour Map of the 'footwall' of the main copper-bearing horizon	60
	13	Graphical plot of a diamond-drill hole log with corresponding titanium and copper values	61
	14	δS^{34} values for pyrite and chalcopyrite	64
	15	Occurrences of Harper Creek-type deposits.	66

LIST OF PLATES

Plate	1	Photograph of fragmental greenstone from Unit 2	26
	2	Photograph of fragmental greenstone from Unit 2	26
	3	Photograph of albite-sericite quartzite from Unit 6a.	27
	4	Photomicrograph of fragmental phyllite from Unit 7 plain polarized light.	27

LIST OF PLATES (Cont.)

			Page
Plate	5	Photograph of fragmental phyllite from Unit 7	27
	6	Photomicrograph of chlorite phyllite, plain polarized light	28
	7	Photomicrograph of chlorite-rich phyllite, plain polarized light	29
	8	Photomicrograph illustrating carbonate prophyroblast partly replaced by sphene, plain polarized light.	29
	9	Photograph of sandy graphitic phyllite from Unit 5 illustrating relation between bedding and S_2.	46
	10	Photograph showing early foliation folded into upright subisoclinal fold	46
	11	Photomicrograph of sandy graphitic phyllite from Unit 5, plain polarized light	47
	12	Photomicrograph showing late slip folds	47
	13	Photomicrograph showing sulphide occurring as replacements of carbonate porphyroblasts, plain polarized light	68
	14	Photomicrograph showing part of a Stage II vein, plain polarized light	68
	15	Photograph illustrating chlorite alteration which imparts a speckeled appearance to some of the rocks	69
	16	Photomicrograph showing chlorite alteration associated with a Stage II vein, cross nicols	69

LIST OF SECTIONS

SECTION	I	8,800E	in pocket
	II	10,000E	in pocket
	III	10,800E	in pocket
	IV	12,060E	in pocket
	V	14,200E	in pocket
	VI	14,500E	in pocket

ACKNOWLEDGMENTS

Financial support for this study was provided by Noranda Exploration Co. Ltd. and by teaching assistantships at the University of B.C.

The writer gratefully acknowledges the assistance given by Dr. A.E. Soregaroli in the selection of the thesis and for his patience and constructive criticisms throughout the completion of the study. Drs. R.B. Campbell and D.J. Tempelman-Kluit from the Geological Survey of Canada and Dr. P.B. Read from the Department of Geology helped with useful discussions. Potassium-argon age determinations were furnished by J.E. Harakal from the Department of Geophysics.

Special thanks go to Miss P. McFeely for her assistance in drafting and to my wife Kathy for her patience and understanding.

Chapter I

INTRODUCTION

The purpose of this study is to investigate the geological setting of the Harper Creek copper deposit, and hopefully, to provide some understanding of the geological evolution of the area.

The field work, on which this study is based, was carried out from 1970 to 1972. Surface mapping was done on a scale of 1 inch equals 400 feet using survey grids, roads and topography for control. Mapping was hampered by both the scarcity and general poor quality of surface exposures.

Location and Accessibility

The Harper Creek copper deposit is located within the Adams Lake Map-Area, British Columbia, at the headwaters of Harper Creek. The city of Kamloops is about 75 miles to the south and the village of Birch Island is located some 7 miles to the northwest (Figure 1).

Access to the region is by the main line of the Canadian National Railway or Highway 5. Both routes follow the North Thompson Valley and pass within 6 miles of the thesis area. The property can be reached by traveling east from Birch Island via a gravel road that follows the south bank of the North Thompson River. About 8 miles from Birch Island, the Jones Creek road is then followed southward for 12 miles to a trailer camp situated at the property.

General Character of the Area

Topography is moderate to steep with elevations ranging from less than 4500 feet to greater than 5700 feet. The area in general is under thick

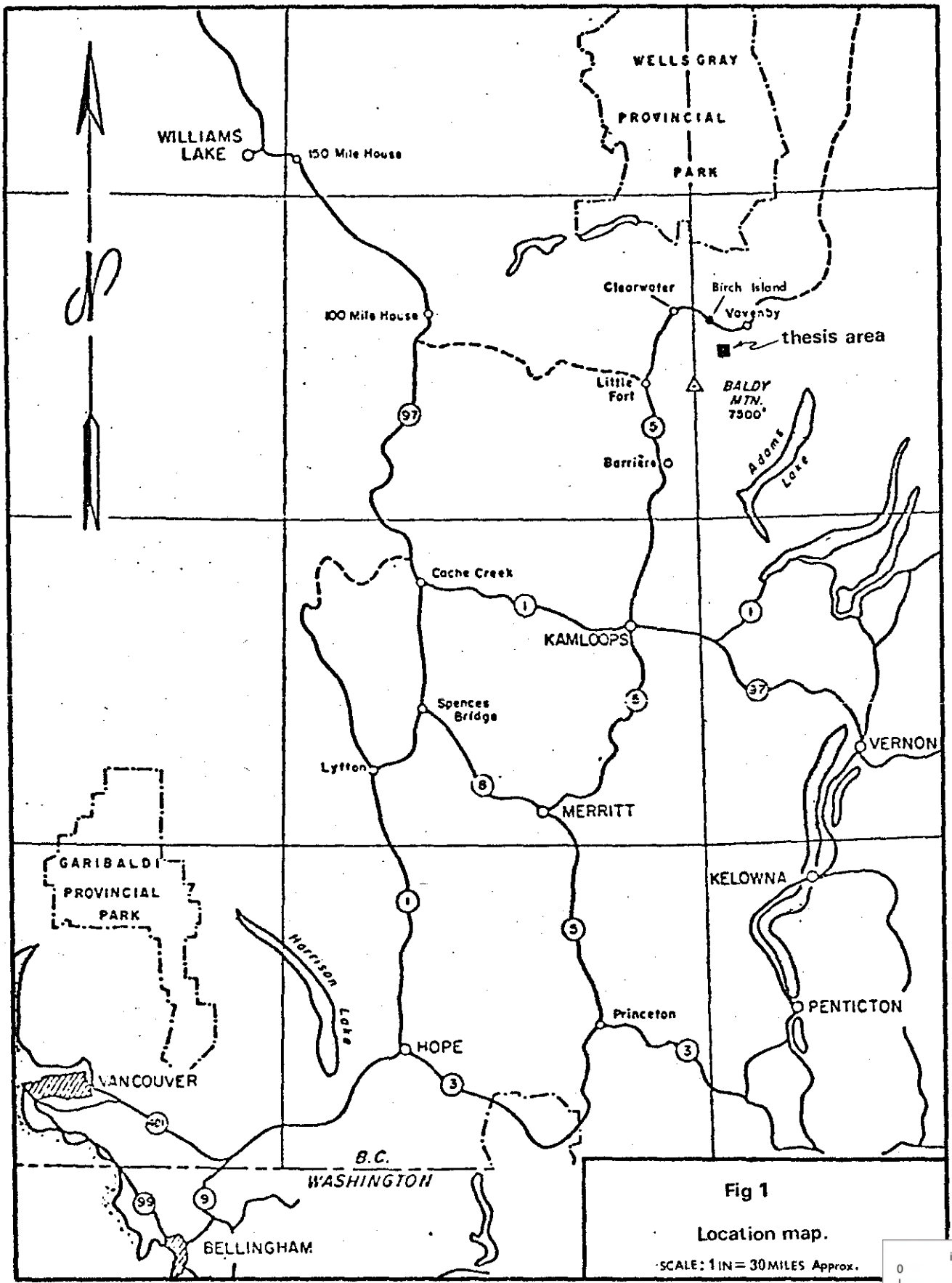

Fig 1

Location map.

SCALE: 1 IN = 30 MILES Approx.

inches
0 1
0 1 2
centimetres
This reference scale bar has been added to the original image. It will scale at the same rate as the image, therefore it can be used as a reference for the original size.
BRITISH COLUMBIA GEOLOGICAL SURVEY

forest cover with heavy underbrush. At higher elevations small marshy alpine meadows prevail. An old forest burn occupies the central and southwest parts of the map-area and to the east many areas have been, or are currently being logged.

History of Development

Part of the deposit was staked by Noranda Exploration Company, Limited in April, 1966 as a result of reconnaissance geochemical work. The ground to the east and south of the Noranda claims was subsequently staked for Quebec Cartier Mining Company, a subsiduary of United States Steel Corporation, in June, 1966. Exploration on the two properties was carried out independently until 1970, at which time a joint venture was formed with Noranda supervising the continued exploration and development.

Exploration techniques employed included soil geochemistry, geophysics, geology, diamond drilling and trenching. To date, more than 9 miles of trenching has been done and some 130 diamond drill holes have been completed.

Chapter II

REGIONAL GEOLOGY

The geology of parts of the Adams Lake and Bonaparte Lake Map-Areas is shown in Figure 2. The most prominent geological feature of the area is a northerly trending belt of highly deformed, metamorphosed Paleozoic and Mesozoic? eugeosynclinal rocks of the Eagle Bay Formation which, together with the rocks of the Shuswap Metamorphic Complex (Monashee Group), define the western limit of the eastern fold belt. This belt is flanked on the west by relatively undeformed and unmetamorphosed Late Paleozoic and Mesozoic eugeosynclinal volcanic and sedimentary rocks. The division between the two provinces is obscure and appears to be gradational.

Rocks of Uncertain Age

Monashee Group

The Monashee Group or Shuswap Metamorphic Complex are part of a series of highly metamorphosed rocks mapped by Dawson (1895) near Shuswap Lake and later named 'Shuswap terrane'. Daly (1912) later examined this same series of rocks along the shores of Shuswap Lakes and Adams Lake.

Rocks of the Monashee Group are highly deformed and metamorphism is generally of sillimanite grade. Gneisses are by far the most common rock types, but amphibolite, quartz-mica schist, quartzite, marble and skarn are locally abundant. In the Adams Lake Map-Area Monashee Group rocks are intruded by a large number of granitic sills, dykes and small stocks.

Eagle Bay Formation

Rocks of the Eagle Bay Formation are equivalent to the Adams Lake and

Fig 2. Geology and mineral deposits of part of the Adams Lake and Bonaparte Lake map-areas; modified from G.S.C. maps 48 1963 and 1278A.

Legend

Cenozoic

QUATERNARY

basalt flows, basaltic cinder cones, basaltic arenite, conglomerate breccia, rubble

TERTIARY

MIOCENE AND/OR PLIOCENE

plateau lava: olivene basalt, basalt andesite, ash, breccia: basaltic arenite

EOCENE AND(?) OLIGOCENE

KAMLOOPS GROUP

Skull Hill Formation: docite, trachyite, basalt, andesite, rhyolite

Chu Chua Formation: conglomerate, sandy shale, arkose, coal

Mesozoic

CRETACEOUS

quartz monzonite, granodiorite, quartz diorite, diorite; minor pegmatite, apilite

JURASSIC

porphyritic augite andesite breccia and conglomerate; minor andesite, arenite, tuff, argillite, flows; siltstone, grit, breccia

TRIASSIC OR JURASSIC

quartz diorite and granodiorite; minor diorite, monzonite, syenodiorite, gabbro, hornblendite

TRIASSIC

NICOLA GROUP

augite andesite and breccia, tuff, argillite, greywacke, grey limestone, shale, phyllite, siltstone

Paleozoic

PENNSYLVANIAN AND PERMIAN

CACHE CREEK GROUP

volcanic arenite, greenstone, argillite, phyllite; minor schist, limestone, basaltic and andesitic flows, amphibolite, conglomerate and breccia

MISSISSIPPIAN AND/OR LATER

Fennel Formation: pillow lava flows, greenstone, greenschist, argillite, chert, limestone, breccia

Proterozoic ?

WINDERMERE OR CAMBRIAN AND LATER

KAZA OR CARIBOO GROUP

feldspathic quartz-mica schist, micaceous quartzite, black siliceous phyllite, marble, chlorite schist, greenstone, amphibolite

Shuswap Terrane

MOUNT IDA GROUP

Eagle Bay Formation: greenstone, greenschist, chlorite schist, phyllite, limestone, quartz-sericite schist, quartzite, volcanic agglomerate, quartz-feldspar-chlorite gneiss, trachytic tuff

marble and limestone; minor greenstone and phyllite

MONASHEE GROUP

gneiss, quartz-mica schist, amphibolite, quartzite, marble, pegmatite

mineral deposits

△ vein and/or fracture mineralization

○ deposit conformable or subparallel with bedding or schistosity

Note: for a description of deposits refer to appendix A

metals

- copper
- molybdenum
- lead, zinc, silver
- gold
- barite, silver
- urananium, rare earths

inches 0 1 0 1 2 centimetres

This reference scale bar has been added to the original image. It will scale at the same rate as the image, therefore it can be used as a reference for the original size.

Niskonlith Series of Dawson (1895) and include the Adams Lake greenstone, Tshinakin limestone and Bastion schist of Daly (1912) as well as the 'Barriere formation' described by Uglow (1922). In the Vernon Map-Area, Jones (1959) mapped the Eagle Bay Formation as part of the Mount Ida Group which he includes in rocks of the 'Shuswap terrane'. In the Adams Lake Map-Area Campbell (1963) divided the Eagle Bay Formation into four unnamed units. On his map they appear as follows:

5. Greenstone, greenschist, chlorite schist, phyllite, limestone, quartz-sericite schist, quartzite, volcanic agglomerate

4. 4a, dark grey and brown phyllite (commonly limy), limestone, sericitic quartzite; minor greenstone, quartz-feldspar-chlorite gneiss, and meta-conglomerate; 4b, trachytic tuff and breccia

3. Grey and buff weathering, white, grey, and buff marble and limestone; minor greenstone and phyllite

2. Undivided; includes rock types common to 4a and 5; minor quartz-mica schist and amphibolite

Because of the close proximity and compositional similarities, the Eagle Bay Formation may include parts of the Cariboo Group, Fennell Formation, Cache Creek Group and Nicola Group.

Serpentinite

Four small masses of serpentinite outcrop within the area of Figure 2 (not shown in Figure 2). Two occur within rocks of the Eagle Bay Formation, one within the Nicola Group and one in contact with rocks of the Thuya batholith. Their age and relation to the surrounding rocks is uncertain.

Proterozoic or Paleozoic

Kaza or Cariboo Group

An area around the eastern end of Mahood Lake, in the Bonaparte Lake Map-Area, is dominantly underlain by quartz-mica schist and micaceous quartzite. Black phyllite, quartz-hornblende-mica schist, marble, chlorite schist and greenstone are also present but in minor amounts. These rocks were mapped by Campbell and Tipper (1971) as part of the Kaza or Cariboo Group.

Paleozoic

Fennell Formation

Dawson (1895) included rocks of the Fennell Formation in the lower part of his Adams Lake Series. These rocks were later described and named the Fennell Formation by Uglow (1922). Campbell and Tipper (1971) correlate the Fennell Formation with the Antler Formation of the Slide Mountain Group.

Aphanitic or very finely crystalline greenstone forms the bulk of the Fennell Formation. Pillow structures are common and at some localities well exposed by railway and highway cuts. Dark grey to black argillite, phyllite and chert are generally restricted to the eastern part of the formation where they occur as beds and lenses interlayered with and intruded by greenstone. At Mahood Lake fine-grained amphibolite and diorite are found with the greenstone.

Cache Creek Group

Dominantly clastic rocks with minor carbonate underlie an area on the west side of the North Thompson Valley in the southwest corner of Figure 2. These rocks were mapped and later described by Campbell and Tipper (1971) as belonging to the eastern part of the Cache Creek Group. Fossil evidence

indicates the rocks range in age from Early Pennsylvanian to Late Permian.

An interesting aspect of this part of the Cache Creek Group is the preponderance of clastic rocks (mainly greywacke and volcanic arenite) and the general absence of chert and thick masses of limestone common to the group elsewhere.

Mesozoic

Two groups of dominantly Upper Triassic rocks have been mapped within the Bonaparte Lake Map-Area. One group, thought to be correlative with the Nicola Group, consists of augite andesite flows with breccia, tuff, argillite, greywacke and grey limestone. Fine-grained clastic rocks, mainly argillite, siltstone and black shale, characterize the second group, but phyllite and black limestone are also abundant.

In the eastern part of the Bonaparte Lake Map-Area, contemporaneous Jurassic rocks have been divided into two units by Campbell and Tipper (1971). One consists of volcanic and clastic rocks with the local development of a basal conglomerate sequence. The other consists of coarse fragmental volcanic rocks in which the fragments are porphyritic augite andesite.

Cenozoic

Kamloops Group

The Kamloops Group includes two formations; 1)a lower sedimentary unit, the Chu Chua Formation and 2)an upper volcanic sequence, the Skull Hill formation.

Chu Chua Formation

Five small areas around Little Fort, in the North Thompson Valley, are underlain by a sequence of conglomerate, sandstone and sandy shale. These

rocks are Eocene in age and unconformably overlie the Fennell Formation. They are apparently conformably overlain by the Upper Eocene to Miocene Skull Hill Formation.

Skull Hill Formation

Acidic to basic volcanic flows, with related breccias, characterize the rocks of the Skull Hill Formation. Individual members include dacite, trachyte, basalt, andesite and rhyolite.

Miocene to Pliocene Plateau Basalt

Many areas of British Columbia are underlain by plateau basalts of Miocene to Pliocene age. Within the Bonaparte Lake Map-Area these rocks are most commonly olivine basalt.

Tertiary? and Quaternary Volcanism

Three periods of Quaternary volcanism are represented in the Bonaparte Lake and Adams Lake Map-Areas. Exposures generally are confined to areas in and around the Wells Gray provincial park. Volcanism was of a basic nature and extended, intermittently, from Pliocene or Pleistocene through to Recent.

Batholithic and Related Rocks

Three large batholiths, the Thuya, Raft and Baldy, which occur within the area of Figure 2, have respective potassium-argon ages of about 195 m.y., 105 m.y. to 140 m.y. and 80 m.y. to 100 m.y. As illustrated in Figure 3, there is a corresponding compositional difference and degree of differentiation with age. Younger rocks trend towards an enrichment in potassium feldspar and quartz relative to plagioclase and tend to be of more variable composition. There is also a decrease in modal percent mafics with decreasing age.

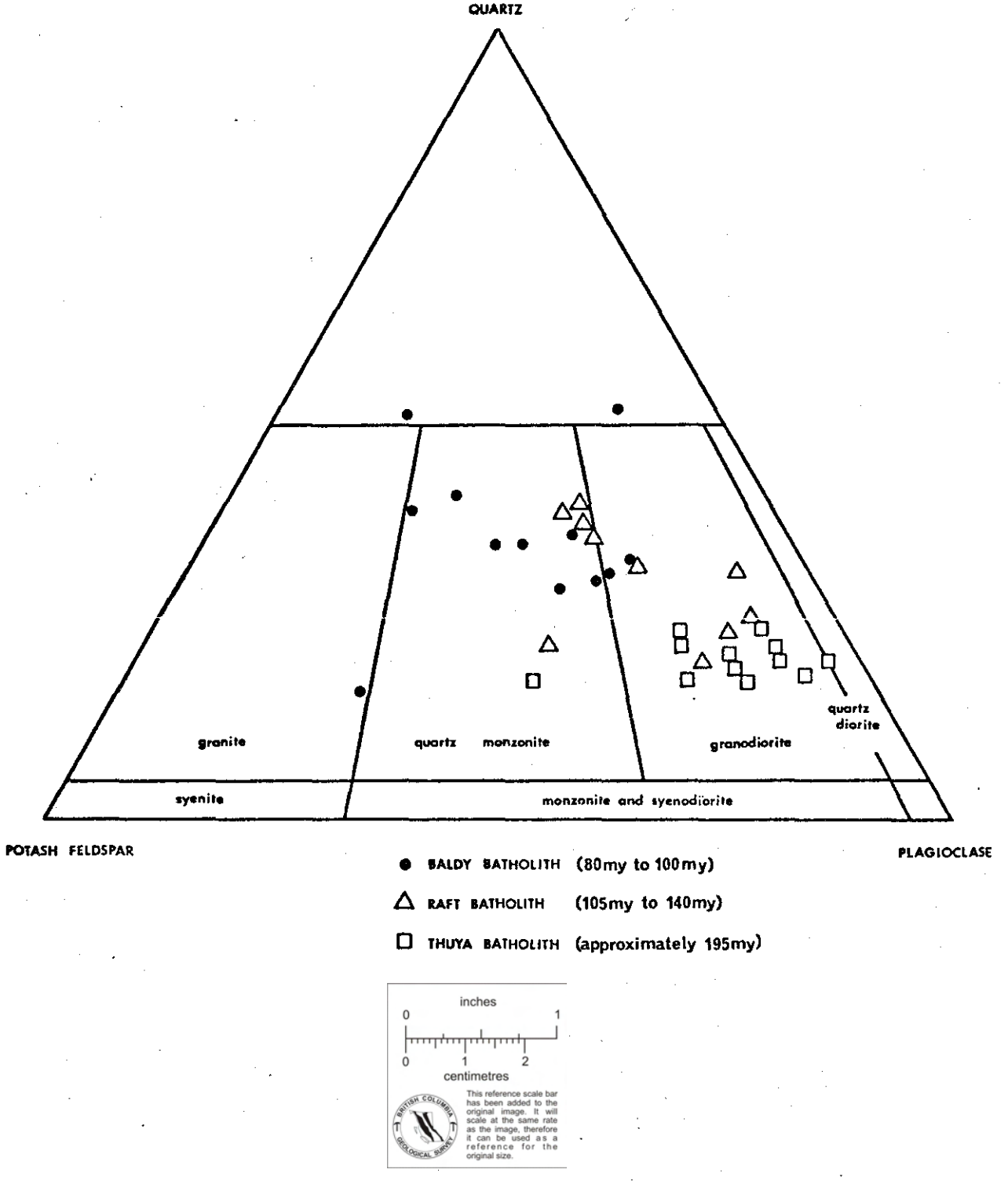

Fig 3. Plot of modal data for Thuya, Raft and Baldy batholiths; modified from G.S.C. memoir 363 pp. 72 and 73.

Chapter III

PETROLOGY

The Harper Creek copper deposit is situated about 2½ miles north of the Baldy batholith (Figure 2). Copper mineralization is confined to tabular-shaped zones within metasedimentary and metavolcanic rocks of the Eagle Bay Formation. The polydeformed host rocks are characteristically well foliated and are locally cut by discontinuous, blocky, altered andesite dykes. Between the Baldy batholith and rocks of the Eagle Bay Formation is a zone of chlorite-biotite gneiss ranging from ½ to more than a mile in width.

Modal distributions for the various map units have been summarized in Table I. The data are at best semiquantitative and in some cases conclusions are drawn from a limited number of observations. Data were drawn from observations made in the field and through the examination of some 70 thin sections. The solid lines represent estimates for probable ranges in values and dotted extensions represent areas of uncertainty. Determinations of albite and potassium feldspar were aided in many cases by etching specimens with cold hydrofluric acid and staining with cobalt nitrate solution. The carbonate is mostly dolomite but the presence of some calcite is indicated from acid tests and X-ray determinations. Pyrophyllite, chloritoid, stilpnomelane and paragonite were not identified in the rocks.

Eagle Bay Formation

Within the map-area, the writer has subdivided the Eagle Bay Formation into 8 petrological map units which are summarized in Table II. For the distribution of these lithologies as well as other map units refer to Figure 4 (in pocket). Cross-Sections I to VI (in pockets) add a third dimension to

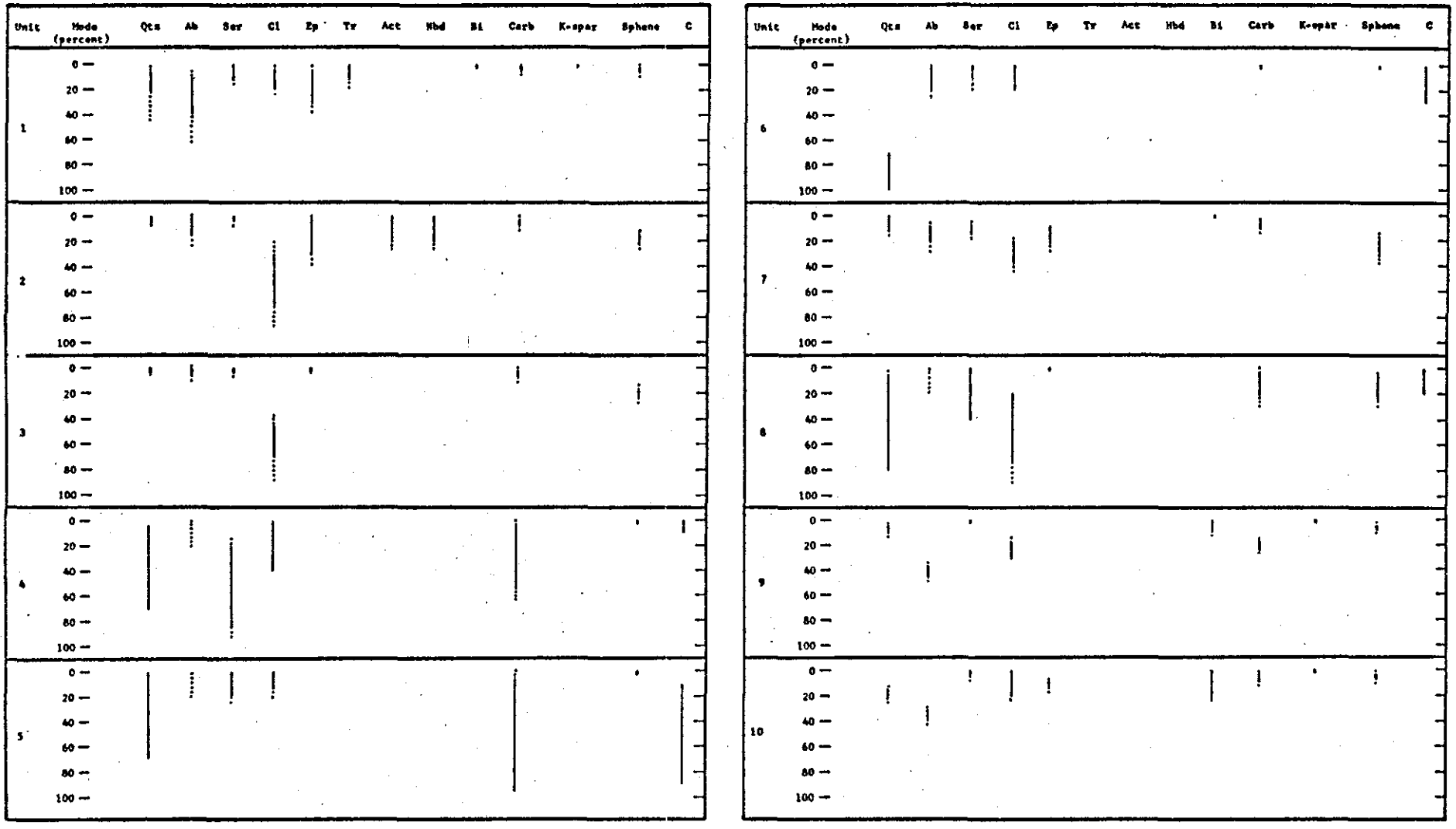

Table 1 Modal Range of Harper Creek Rocks.

the perspective.

Unit	General Lithology	Source Rock(s)
1	Quartzo-feldspathic phyllite (locally well laminated); minor light green, laminated greenstone	Acidic flows? and/or tuffs?
2	Foliated, fragmental greenstone; chlorite phyllite	Basic tuff; locally with abundant hornblende and/or acidic volcanic fragments
3	Chlorite phyllite	Basic tuff
4	White to light green, well-foliated, lustrous phyllite	Marls, sandy shales, argillaceous arenites; locally tuffaceous
5	Graphitic and carbonaceous phyllite; minor dolomite	Carbonaceous arenites, carbonaceous shales, carbonaceous carbonates and carbonaceous marls; locally tuffaceous
6	6a Orthoquartzite, sericite quartzite, albite-sericite quartzite	Quartz arenite, feldspathic arenites, argillaceous feldspathic arenites; locally tuffaceous
	6b Carbonaceous quartzite	Carbonaceous arenites; locally tuffaceous
7	Dark green fragmental phyllite	Pebbly tuffaceous greywacke
8	Chlorite phyllite, quartz-chlorite-sericite phyllite, chlorite-sericite phyllite; minor chlorite quartzite	Basic tuff and tuffaceous sediments

Table II General Lithologies of the Eagle Bay Formation, Harper Creek.

Unit 1

Pale to light green quartzo-feldspathic phyllite forms the bulk of Unit 1. The phyllite averages about 75 percent quartz and feldspar, 10 percent chlorite, 8 percent clinozoisite, 4 percent sphene and contains minor amounts of carbonate and sericite. The feldspar is albite and generally occurs as

anhedral untwinned grains. Chlorite and clinozoisite occur finely disseminated throughout the rock.

The phyllite is homogeneous but locally well laminated. Laminae consist of chlorite and clinozoisite-chlorite-rich layers within a dominantly quartzo-feldspathic rock. Laminae are discontinuous, contorted and generally less than one centimeter in thickness. The clinozoisite-chlorite-rich laminations are fine grained and contain, in addition to clinozoisite and chlorite, up to 20 percent sericite, about 5 percent quartz and feldspar, 5 percent sphene and minor amounts of tremolite and carbonate. Some larger laminae contain very fine laminations of sphene and clinozoisite.

Locally, Unit 1 consists of light green, laminated greenstone. The greenstone contains about 30 percent fine-grained clinozoisite, 35 percent albite, 10 percent tremolite, 10 percent chlorite, 5 percent carbonate, 5 percent quartz and 4 percent sphene. Tremolite occurs as fine slender acicular crystals within quartz and feldspar and as coarser prismatic laths in laminations with clinozoisite and chlorite. Most of the feldspar and quartz is very finely crystalline, equigranular and anhedral. Porphyroblasts of albitic plagioclase are restricted to coarser grained pods and laminations.

Unit 2 locally contains greenstone fragments which resemble some of the rocks of Unit 1. These fragments have partly preserved phenocrysts of hornblende and feldspar and appear to be of volcanic origin.

Unit 2

Foliated, fragmental greenstone and chlorite phyllite, mapped as Unit 2, outcrop over a small area north of the Noranda camp. The greenstone is medium to dark green and contains angular to subrounded hornblende and/or greenstone

fragments up to 1 inch across (Plates 1 and 2). Hornblende fragments exhibit various degrees of alteration to chlorite with lesser and variable amounts of epidote, actinolite and carbonate. Most hornblende fragments are part of single hornblende crystals and have sheared chloritized margins. Some hornblende has partly preserved crystal outlines and some contain euhedral albite grains up to 2 mm in size. Greenstone fragments consist of 50 percent fine-grained clinozoisite evenly distributed within a very finely crystalline quartz-feldspar groundmass. Small, subhedral to euhedral hornblende phenocrysts, which are partly altered to clinozoisite and chlorite, and feldspar phenocrysts pseudomorphed by carbonate are also evident.

Chlorite phyllite and the matrix of the fragmental greenstone are fine grained and well foliated. Where hornblende fragments are present, the matrix consists of actinolite, clinozoisite, feldspar, chlorite, sphene, carbonate and quartz. Fine acicular to lath-shape actinolite occurs oriented in the plane of the foliation but coarser actinolite occurs as laminations parallel to and cross-cutting the foliation. Clinozoisite is characteristically fine grained and evenly distributed. Albitic plagioclase occurs as very fine, anhedral, untwinned grains interstitial to other minerals. Sphene is abundant and occurs as fine disseminations in amounts up to 20 percent. Chlorite phyllite and greenstone of Unit 2 without hornblende fragments contain about 70 percent chlorite and 20 percent sphene with less than 5 percent feldspar and less than 2 percent clinozoisite.

The textures and composition of the chlorite phyllite and the matrix of the greenstone of Unit 2 suggest that these rocks may have originally been basic tuffs. Hornblende and greenstone fragments possibly represent volcanically ejected material which were incorporated into the tuff.

Unit 3

Dark green chlorite phyllite, assigned to Unit 3, has a uniform appearance and weathers a dull, dark green color. This phyllite, which is virtually the same as the chlorite phyllite of Unit 2, contains chlorite in excess of 50 percent plus sphene, quartz, feldspar, carbonate and minor clinozoisite. Sericite is present in some of the rocks. Sphene, as in the rocks of Unit 2, is abundant and present in amounts up to 20 percent.

Unit 4

Unit 4 consists of white to light green, well-foliated, lustrous phyllite. Varieties of phyllite, based on the relative abundancies of quartz, albite, sericite, chlorite and carbonate, include: sericite-carbonate, sericite, quartz-sericite, quartz-sericite-chlorite and sericite-chlorite phyllite. The stratigraphic relation of these phyllites is unknown but they commonly occur interstratified as lenses and discontinuous layers with gradational contacts. Varieties of phyllite, which generally are less than 50 feet in thickness, may be repeated several times in a drill hole and there is no observed systematic vertical or lateral variation within the phyllites. Correlation of varieties of phyllite of Unit 4 between diamond drill holes or from one outcrop to the next often was not possible.

The phyllite of Unit 4 is texturally diverse. All rocks are well foliated with a well-developed cleavage. Most are fine grained but many contain small pods and laminations of coarser grained material. Many rocks are thinly laminated and readily split into thin sheets. Laminations, which consist of quartz-and feldspar-rich segregations, separated by a thin layer of soft phyllite, parallel the foliation. Some phyllite contains porphyroblasts of quartz, carbonate and albite. Porphyroblasts of quartz are most common and occur as clear rhombohedral, spherical and eye-shaped grains up to ½ inch across.

The phyllite of Unit 4 probably was derived from marls, sandy shales and argillaceous arenites. A corresponding increase in sphene with increasing chlorite content of some of the rocks of Unit 4 suggests the source of titanium may be the same as for the sphene-rich chlorite phyllites of Units 2 and 3 (i.e. basic tuff).

Unit 5

Dark grey to black, graphitic and carbonaceous phyllite, mapped as Unit 5, occurs as scattered lenses and discontinuous, irregular-shaped bodies. The phyllite contains more than 30 percent graphite and carbonaceous matter. Sericite is usually less than 10 percent and carbonate varies from less than 2 percent to more than 20 percent. Quartz content varies from less than 5 percent to 70 percent. Chlorite, although generally absent, is present in some of the rocks.

Fine-to medium-crystalline, grey dolomite occurs as discontinuous tabular bodies within graphitic and carbonaceous phyllite. Dolomite beds generally are less than 2 feet and no more than 50 feet in thickness.

Unit 6

Small outcrops of quartzite (Unit 6) occur scattered throughout most of Units 4 and 5. Outcrops of quartzite, which are too small to record at the map scale, occur as isolated, resistant knobs within recessive-weathering phyllite. Quartzite forms bluffs along the north bank of Harper Creek near the centre of the map-area. In some areas, quartzite occurs as thin beds interstratified with phyllite. Exposures containing more than 50 percent quartzite were mapped as part of Unit 6.

Unit 6 is divided into 2 units based on the presence or absence of

visible carbonaceous matter.

Unit 6a

Unit 6a consists of orthoquartzite, sericite quartzite and albite-sericite quartzite. The rocks are white to light green, hard and resistant. Orthoquartzite contains more than 95 percent quartz as anhedral, tightly interlocking grains. Within the albite-sericite quartzite and to a lesser extent within the sericite quartzite detrital grains are partly preserved (Plate 3). These rocks contain sand-size, angular to well-rounded quartz and feldspar grains in a fine-grained, quartzo-feldspathic groundmass. Sericite occurs between sand grains and along cleavage planes.

Unit 6b

Unit 6b consists of carbonaceous quartzite. Most carbonaceous matter occurs between framework grains but locally fills fractures cutting framework grains. Original clastic textures, as in the rocks of Unit 6a, often are preserved.

Unit 7

Resistant, dark green, fragmental phyllite, mapped as Unit 7, forms a prominent east-west ridge some 2000 feet in length extending into the western part of the map-area. Light-colored, well-rounded fragments, which comprise about 50 percent of the phyllite, occur evenly distributed within a dark green, fine-grained, well-foliated matrix (Plate 4). Most fragments are 1 mm to 2 mm across but range from less than 0.1 mm to greater than 5 mm. Stratigraphic variance in fragment size has the appearance of graded bedding (Plate 5). Fragment shape varies from irregular spheres to lenticular. Lenticular grains define a good lineation by their preferred orientation in the plane of the

foliation. Most fragments are polymineralic with variable amounts of epidote, carbonate, quartz, feldspar, chlorite and sericite. An average fragment contains approximately 30 percent albite, 20 percent epidote, 15 percent carbonate, 15 percent quartz, 10 percent chlorite, 5 percent sericite and minor sphene. The fine-grained, well-foliated matrix surrounding fragments consists of about 40 percent chlorite, 40 percent sphene, 10 percent sericite, 5 percent quartz and feldspar and 5 percent epidote. Very fine-grained sphene occurs as disseminations and in clusters which locally exceed 80 percent of the matrix.

Unit 7 may represent the metamorphosed equivalent of a tuffaceous pebbly greywacke. Fragments appear to have been detritus from a volcanic source. The chlorite-sphene matrix possible was derived from basic tuffaceous material.

Unit 8

Unit 8 consists of medium to dark green, chlorite phyllite, quartz-chlorite-sericite phyllite and chlorite-sericite phyllite with minor amounts of medium to dark green chlorite quartzite. The phyllites generally occur interstratified as lenses and discontinuous layers with gradational contacts. Chlorite phyllite of Unit 8 is the same as the chlorite phyllite of Units 2 and 3. Textures of quartz-chlorite-sericite phyllite and chlorite-sericite phyllite resemble those of the phyllites of Unit 4. Distinction between the units is based on the greater amount of chlorite present within the phyllites of Unit 8. As in the phyllites of Unit 4, there is a corresponding increase in sphene with increasing chlorite content.

Textures and the general association between sphene and chlorite suggest the rocks of Unit 8 were originally basic tuffs and tuffaceous sediments.

Unit 8 apparently forms a gradational series between Units 3 and 4.

Metamorphism of Units 1 to 8

Metamorphic minerals present within Units 1 to 8 include: quartz, albite, sericite, chlorite, sphene, carbonate, epidote, tremolite and actinolite; an assemblage characteristic of the quartz-albite-muscovite-chlorite subfacies of the greenschist facies of regional metamorphism.

Deformation, which accompanied regional metamorphism, was characterized by the development of a strong crenulation foliation which transposed bedding and an earlier foliation. It was not determined whether the earlier foliation is part of the same metamorphic event or indicates an earlier metamorphic episode. Deformation appears to have outlasted metamorphism.

Equilibrium was not always attained during regional metamorphism; thin sections of hornblende-bearing lithologies from Unit 2 reveal the hornblende weakly to intensely altered to chlorite, epidote, actinolite and carbonate.

Titanium

Sphene, as previously noted, is a major constituent of parts of Units 2, 3, 7 and 8. Within these units, chlorite-rich phyllite is the principle host for sphene. The fine grain size, basic composition, abundance of sphene and the lack of volcanic textures suggest this phyllite was originally a titanium-rich basic tuff.

Most sphene occurs evenly disseminated or in clusters which appear opaque in thin section (plain polarized light) (Plate 6). By insertion of the condensing lens, opaque grains of sphene can be resolved as clusters of minute, highly birefringent, anhedral to euhedral sphene crystals, many of which have dull brown leucoxene? halos. This sphene appears to have formed during

regional metamorphism and at least some occurs as partial replacements of clinozoisite (Plate 7).

Some sphene occurs as replacements of carbonate in the matrix of phyllite and as partial to complete replacements of carbonate porphyroblasts (Plate 8). Sphene of this character appears to post-date regional metamorphism and generally is within and adjacent to areas of suphide mineralization, which suggests a hydrothermal origin for the sphene.

'Hydrothermal sphene' is coarser grained than sphene formed during regional metamorphism and is not opaque in thin section (plain polarized light). In hand specimen, 'hydrothermal sphene' is buff to orange colored.

Unit	Description	a.Titanium (weight percent)	b.Estimated Sphene (volume percent)	Ratio a:b (approximate)
2	Fragmental greenstone (hornblende fragments)	1.92	20	1:10
3	chlorite phyllite	1.20	15	1:12
7	fragmental phyllite	2.77	+20	1:7
8	chlorite phyllite	1.92	20	1:10
8	chlorite phyllite	2.29	+20	1:9

Table III Titanium Values of Some Eagle Bay Rocks, Harper Creek

Titanium values obtained for Units 2, 3, 7 and 8 as well as the estimated volume of sphene for the rocks assayed are shown in Table III. Rocks assayed for titanium contained little or no 'hydrothermal sphene'.

Table III also shows the estimated titanium: sphene ratios. Although there is no pretense that these estimates are accurate, they probably illustrate

significantly higher ratios than for pure sphene which would indicate a large substitution for titanium within the lattice structure of sphene formed during regional metamorphism (titanium: sphene ratio for pure sphene is about 1:4). This assumption is supported by petrographic, X-ray and polished section studies. In polished sections, under reflected light, sphene formed during regional metamorphism varies from yellow to dark red to steel metallic. Yellow and red varieties display respective bright yellow and bright red internal reflections. X-ray traces of this sphene show a difference, by as much as 1 degree, in the 2θ position of the $00\overline{2}$ peak.

Age and Distribution of the Eagle Bay Formation

The Eagle Bay Formation underlies a large part of the western half of the Adams Lake Map-Area and extends south into the adjoining Vernon Map-Area where it was mapped as part of the Mount Ida Group by Jones (1959). The only fossil locality discovered within this formation has yielded conodonts of Middle Mississippian age (Campbell, personal communication). While much of the formation may be of this age, it possibly includes younger and/or older strata.

Andesite Dykes (Unit 9)

Dykes of altered andesite, mapped as Unit 9, were intersected in some diamond-drill holes. The dykes have chilled margins and locally incorporate fragments of phyllite. Although the cores of the dykes are relatively undeformed the margins are sometimes sheared and locally well brecciated.

Most of the dykes are porphyritic (plagioclase phenocrysts) and have a dark grey to green, fine-grained, pandiomorphic granular matrix. The dykes contain approximately 40 percent albite, 20 percent carbonate, 30 percent chlorite and biotite, 5 to 10 percent quartz, 3 percent sphene and minor

amounts of potassium feldspar and sericite. Thin sections of andesite dyke reveal biotite weakly to intensely altered to chlorite. Some of the chlorite contains finely disseminated sphene. Carbonate occurs as patches and clusters of grains within and around polysynthetically twinned, tightly interlocked albite.

The orientation of the dykes in the map-area is not precisely known because they have generally been observed only in drill core. One andesite dyke, south of the map-area, was observed to have a vertical dip and a northerly strike.

Chlorite-Biotite Gneiss (Unit 10)

Chlorite-biotite gneiss, designated as Unit 10, underlies a small area in the southwest corner of the map-area. This fine-to medium-grained, moderately well-foliated gneiss contains approximately 35 percent albite, 20 percent quartz, 20 percent chlorite and biotite, 10 percent epidote and clinozoisite, 5 percent carbonate and 5 percent sphene. Albite normally is anhedral and untwinned. Chlorite occurs as an alteration of brown, pleochroic biotite.

Chlorite-biotite gneiss, the same as Unit 10, outcrops south of the map-area. Here, the foliation in the gneiss appears to define a large east-west oriented antiform, the core of which is occupied by the Baldy batholith. Foliation in the gneiss south of the batholith dips 20 to 60 degrees south whereas foliation in the gneiss north of the batholith dips 20 to 60 degrees north.

The contact between gneiss and rocks of the Eagle Bay Formation is

marked by an increase in the degree of foliation in the gneiss and locally by the appearance of biotite and/or actinolite as fracture coatings and disseminations in rocks of the Eagle Bay Formation. With increasing distance from the contact, the gneiss is less foliated and locally displays a hypidiomorphic-granular texture. Albite often is euhedral, well twinned and tightly interlocked with quartz. At the headwaters of Foghorn Creek, about 5 miles west of Harper Creek, the gneiss contains pods, up to 10 feet across, of unfoliated quartz diorite. Within the quartz diorite, mafic minerals are partly to completely chloritized.

Metamorphism of Unit 10

Prograde metamorphic minerals within Unit 10 include: quartz, albite, biotite, muscovite, microcline, epidote, carbonate and sphene. The coexistence of albite and epidote and the presence of biotite limit metamorphism to either the quartz-albite-epidote-biotite or the quartz-albite-epidote-almandine subfacies of the greenschist facies of regional metamorphism. The lower-grade quartz-albite-epidote-biotite subfacies is favored because of the absence of almandine garnet and because twinning in plagioclase, which tends to be destroyed during metamorphism, is still prevalent in some of the rocks.

Retrograde metamorphism of the gneiss has resulted in partial to complete chloritization of biotite.

Biotite and actinolite in rocks adjacent to the gneiss is seemingly anomolous because these minerals are younger than the regional metamorphism which affected these rocks. The following model is suggested to explain this anomaly:

Both the gneiss and rocks of the Eagle Bay Formation were affected

> by the same period of metamorphism. Near the end of metamorphism isotherms were lowered and metamorphism ceased in the upper, lower-grade metamorphic zones. At this time the gneiss, which was still hot, was folded and squeezed into the cooler overlying strata. This movement of hot gneissic rocks into rocks of lower metamorphic grade resulted in the raising of isotherms and the partial readjustment of the contact rocks to the new temperature conditions.

Therefore, using this interpretation, the contact between the gneiss and rocks of the Eagle Bay Formation may, in part, represent a faulted biotite isograd.

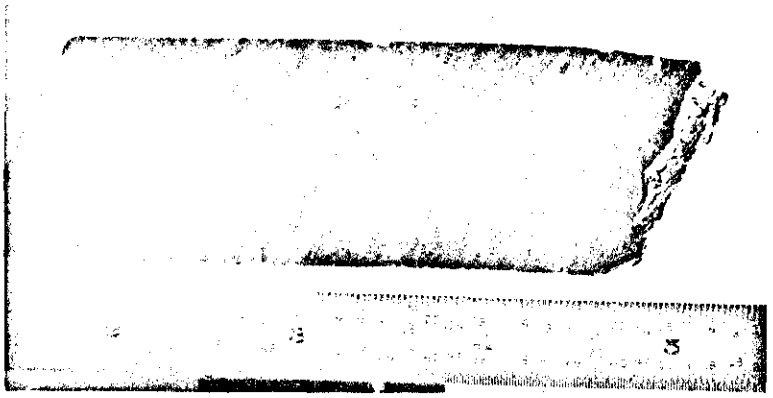

Plate 1 Photograph of fragmental greenstone from Unit 2. Dark fragments are partly altered hornblende and the matrix surrounding fragments consists largely of actinolite, clinozoisite, chlorite, sphene and carbonate. The scale is in inches.

Plate 2 Photograph of fragmental greenstone from Unit 2. Fragments are light green greenstone and appear to be of volcanic origin. The phyllite surrounding greenstone fragments is largely composed of chlorite and sphene. The scale is in inches.

Plate 3 Photograph of albite-sericite quartzite from Unit 6a. Note the sand size grains, their roundness and apparent well-sorted nature. The scale is in inches.

Plate 4 Photomicrograph of fragmental phyllite from Unit 7, plain polarized light. Fragments are mainly composed of epidote, quartz, albite and carbonate. The dark matrix surrounding fragments is mainly sphene.

Plate 5 Photograph of fragmental phyllite from Unit 7. Note the smaller fragment size toward the top of the specimen. The scale is in inches.

Plate 6 Photomicrograph of chlorite phyllite, plain polarized light. Sphene appears as opaque patches.

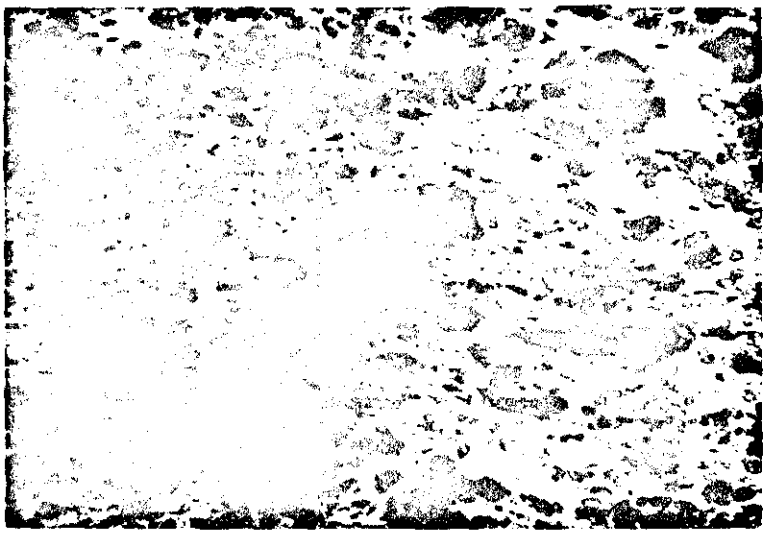

Plate 7 Photomicrograph of chlorite-rich phyllite, plain polarized light. Sphene appears opaque on the photo and apparently replaces clinozoisite (light grey, high relief grains).

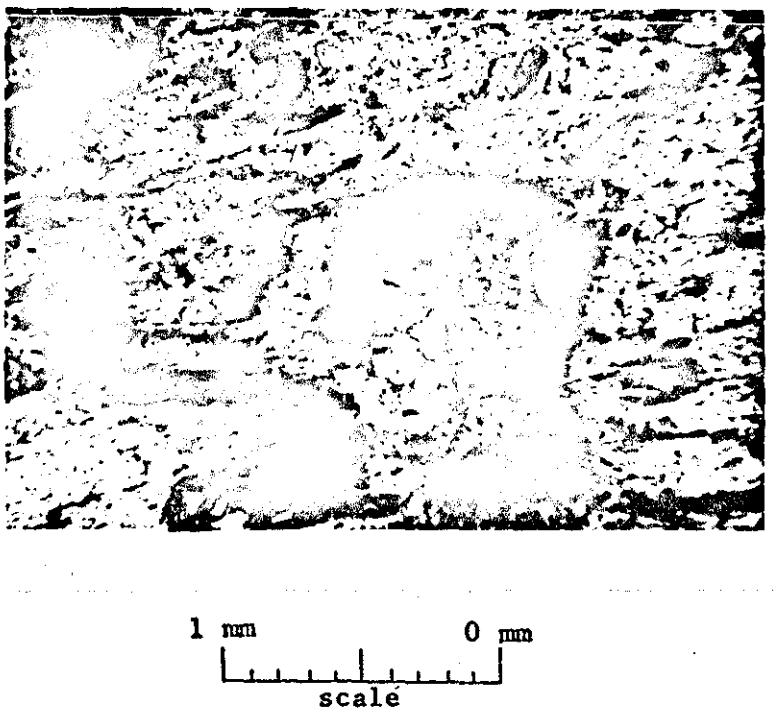

Plate 8 Photomicrograph showing carbonate porphyroblast (right-center of photo) partly replaced by sphene (dark rim around porphyroblast), plain polarized light. Dark vein-like areas on photo consist of chlorite and sphene.

Chapter IV

STRUCTURE

Interpretation of the structural history of the Harper Creek area is difficult because of complex structure, scarcity and general poor quality of surface exposures and locally, by the superimposition of later hydrothermal events.

Eagle Bay Formation

Small-scale structures, which include foliations, lineations, folds and fractures, are well developed within the Eagle Bay Formation. Large-scale structures, notably folds, exist but are not readily apparent because of complex structure and similarity of many lithologies.

Some of the data pertaining to the orientation of various structures are plotted on schmidt equal-area nets (lower hemisphere projections) and appear as Figures 6 to 9. Fold axis and fracture data were supplemented by data collected by others (Kirkland, 1971; Westerman, 1968).

Small-Scale Structures

Foliations

The earliest recognizable foliation, S_1, is parallel to subparallel to bedding. Where evident, this foliation commonly occurs as microscopic quartz-rich and/or mica-rich laminations.

Bedding and S_1 have been transposed by a well developed crenulation foliation, S_2. The latter, which dips uniformly to the north-northwest at about 30 degrees (Figure 6), was formed by slippage along irregular-spaced,

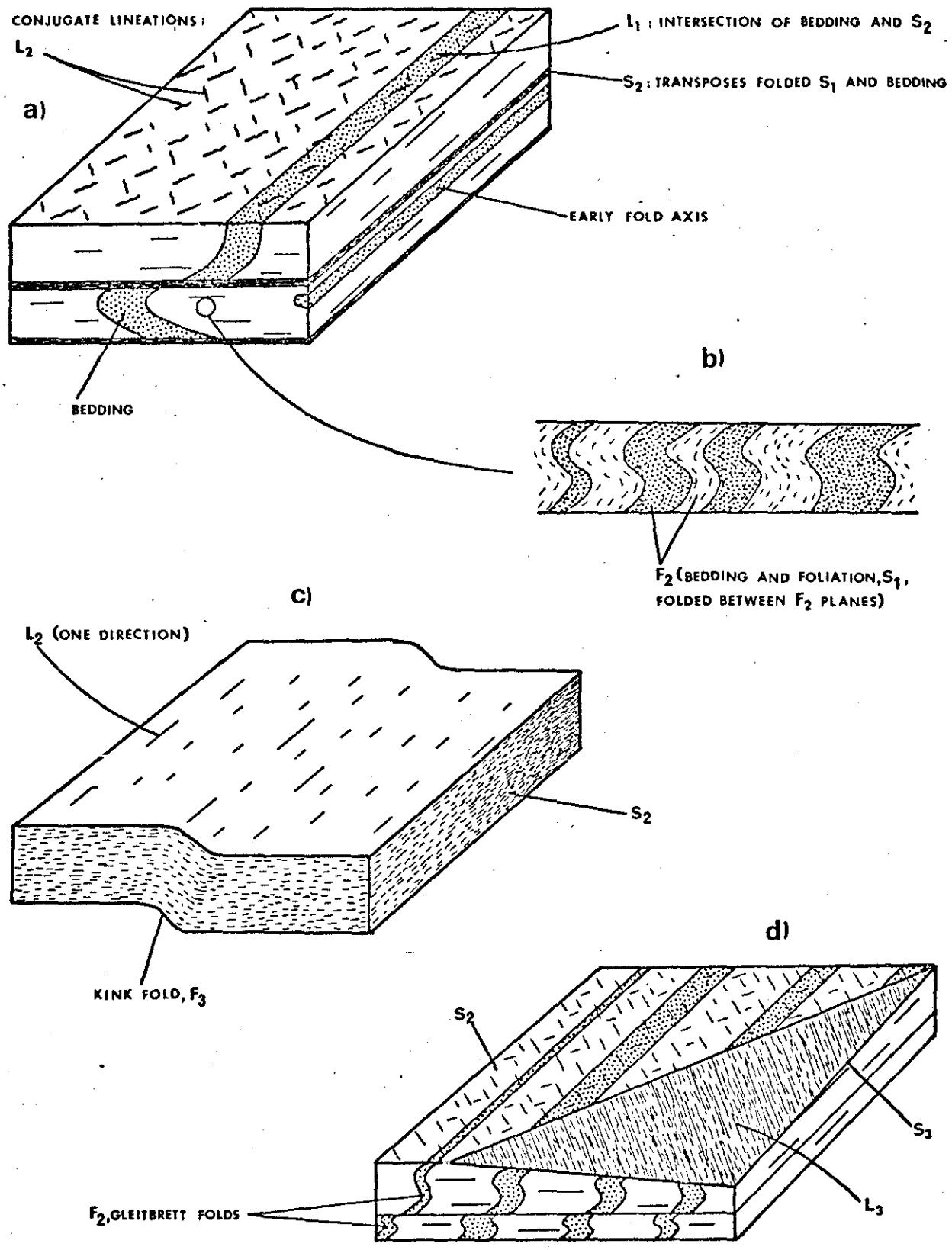

Fig 5. Schematic diagram to illustrate structures in rocks of the Eagle Bay Formation.

inches
0 1
0 1 2
centimetres
This reference scale bar has been added to the original image. It will scale at the same rate as the image, therefore it can be used as a reference for the original size.

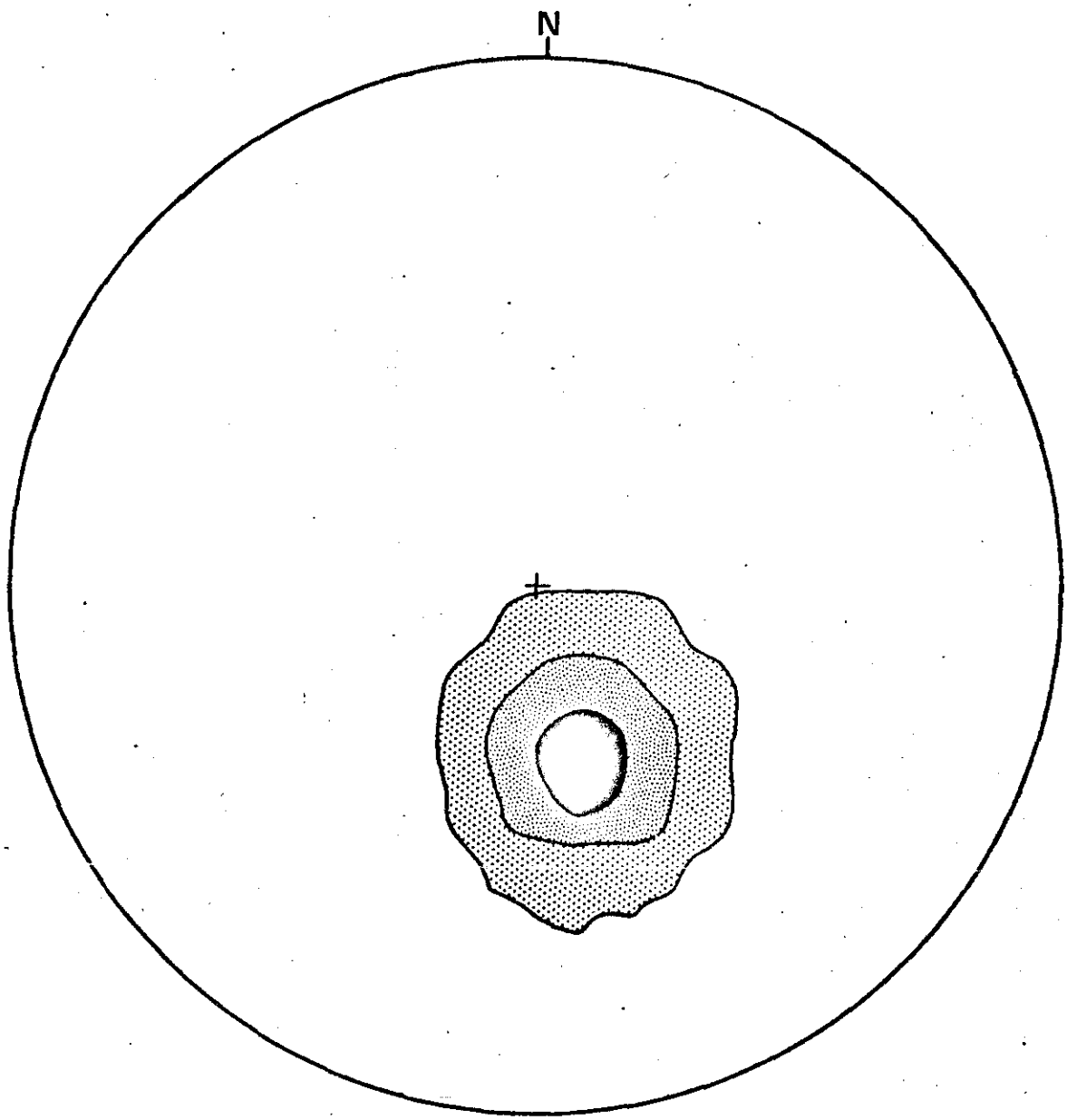

PER ONE PERCENT AREA

1 – 10%

10 – 30%

> 30%

Fig 6. Plot of poles to S_2 (144 plotted).

inches
0 1
0 1 2
centimetres
This reference scale bar has been added to the original image. It will scale at the same rate as the image, therefore it can be used as a reference for the original size.

parallel zones up to 2 mm in thickness. Formation of S_2 was accompanied by incipient crystallization of micas parallel to S_2 and was followed by total recrystallization where transposition was complete. Deformation appears to have outlasted crystallization.

Slickensided surfaces, designated as S_3, were developed subparallel to S_2 (Figure 5d). These surfaces (S_3), which post-date S_2, are only locally evident.

Linear Structures

The intersection of S_1 or bedding with S_2 defines a linear structure, L_1. This lineation appears on S_2 surfaces as faint lines or bands (Figure 5a), which plunge northerly. The fold crests of minute gleitbret folds developed between S_2 planes (Figure 5b) occasionally define another lineation which parallels L_1, and also will be refered to as L_1.

Wrinkle lineations are well-developed on S_2. These lineations, which are designated L_2, have the form of very small folds which typically are asymmetric and discontinuous. Wrinkle lineations, which plunge to the northeast and northwest parallel to S_2 (Figure 7), have apparently formed as a conjugate set (Figures 5a and 7). Northwest-plunging wrinkle lineations are ubiquitous and often the only lineation present. Northeast-plunging wrinkle lineations are only locally evident.

A third lineation, L_3, occurs as striations on S_3 surfaces (Figure 5d). This lineation is subparallel to northwest-plunging wrinkle lineations and indicates a northwest direction of movement.

Other linear structures include mullions, quartz rods, boudin and

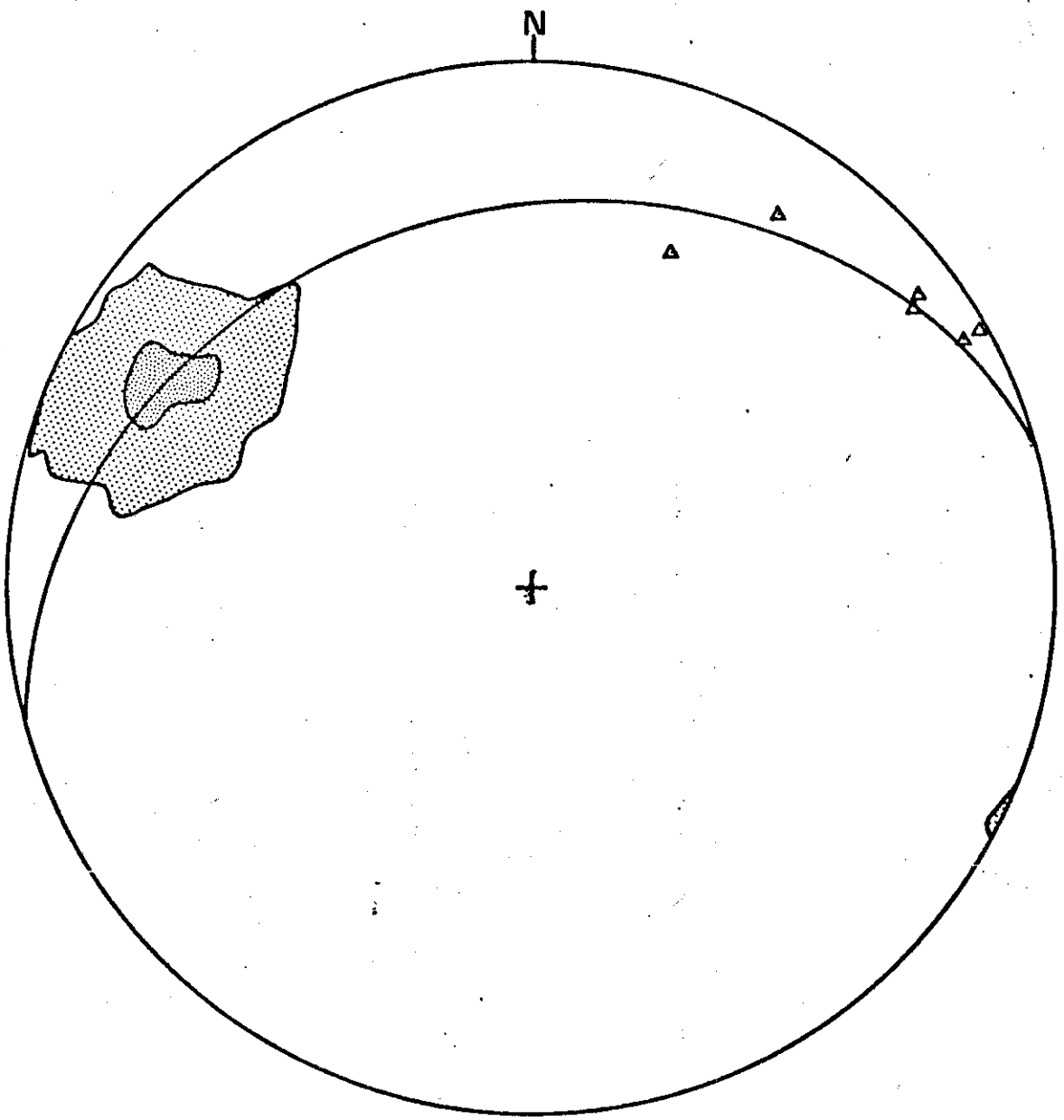

PLOT OF NORTHWEST-PLUNGING WRINKLE LINEATIONS, CONTOURED, 66 PLOTTED

PER ONE PERCENT AREA

5 – 25%

>25%

△ PLOT OF NORTHEAST-PLUNGING WRINKLE LINEATIONS, 6 PLOTTED

Fig 7. Plot of northwest- and northeast-plunging wrinkle lineations and average great circle for S_2.

inches
0 1
0 1 2
centimetres
This reference scale bar has been added to the original image. It will scale at the same rate as the image, therefore it can be used as a reference for the original size.

stretched pebbles, all of which parallel L_1.

Folds

Small-scale folds are not abundant within the Eagle Bay Formation and many are not visible to the unaided eye. Folds earlier than those which deform S_1 are not evident.

Asymmetric, S-shaped, gleitbret folds, designated as F_2, deform bedding and S_1 and have developed by transposition between S_2 planes (Figures 5b and 5d). These folds, which have fold axes defined by L_1 and axial planes parallel to S_2, generally have amplitudes less than 1 cm and show a relative sense of movement of east to west.

Gleitbret folds locally were preceded by the development of small-scale, subisoclinal folds, F_1. Subisoclinal folds display transposition along S_2 (Plates 9, 10 and 11) and appear to have developed as an early structure during the same deformation which produced S_2 and F_2. F_1 folds have attenuated limbs, interlimb angles between 10 and 30 degrees and plunge northerly approximately parallel to F_2. Most are reclined with axial planes parallel to S_2, but some were observed in an upright position.

Locally, phyllites display kink folds, F_3, which deform S_2 (Figure 5c). These folds developed as a conjugate set with amplitudes less than 10 cm and the same axial orientations as the conjugate L_2 wrinkle lineations (compare Figures 7 and 8). Geometry of kink folds suggests an overall sense of movement from south to north with one limb parallel to S_2 and the other limb dipping steeply to the northeast or northwest. Northwest-plunging kink folds are better developed and on occasion both sets are exposed within the same outcrop. Development of kink folds was accompanied by renewed slippage

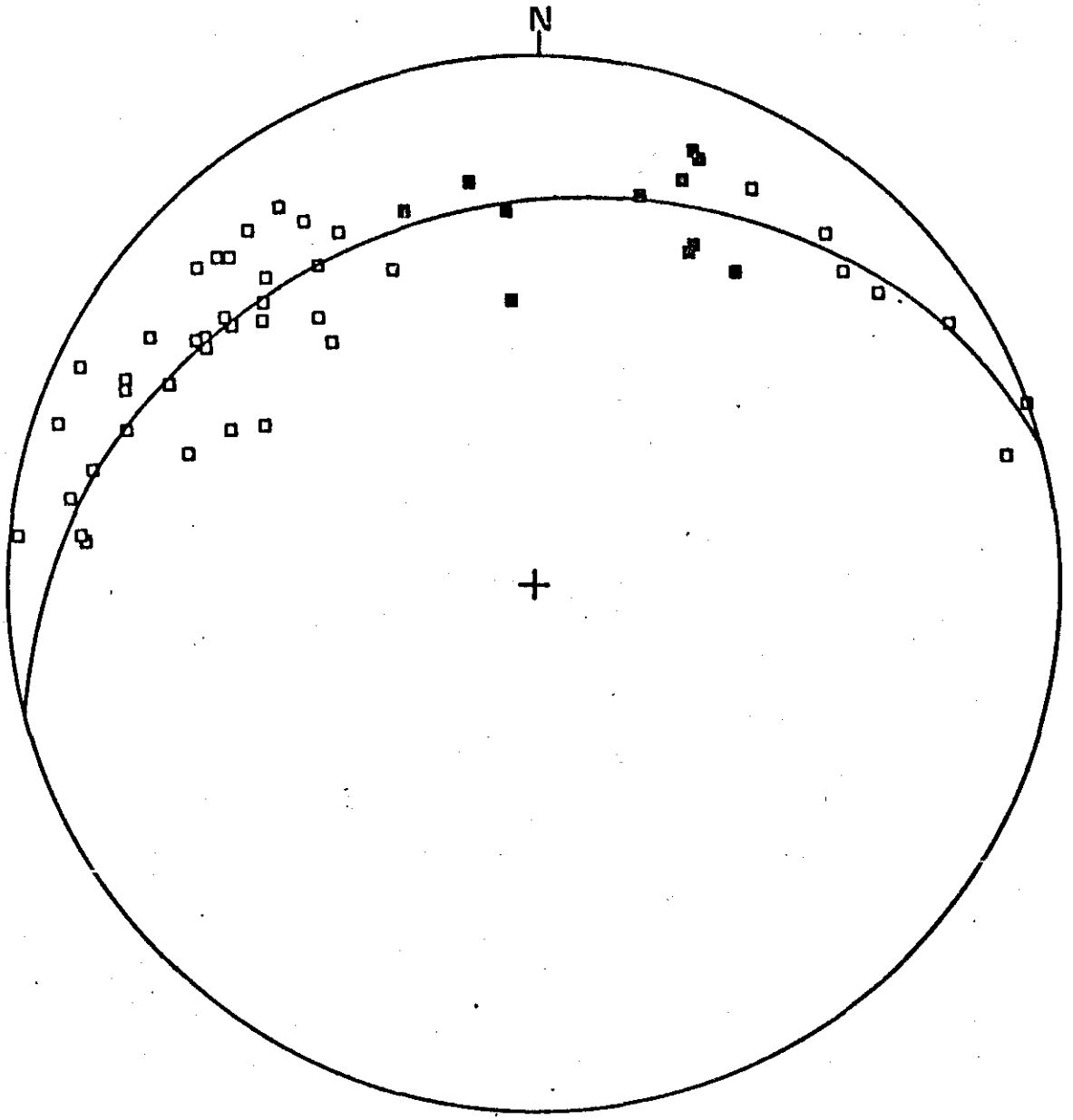

Fig 8. Plot of early and late (kink and open) fold axes and average great circle for S_2.

inches
0 1
0 1 2
centimetres
This reference scale bar has been added to the original image. It will scale at the same rate as the image, therefore it can be used as a reference for the original size.

along S_2.

Conjugate open folds, which are co-axial with kink folds, are locally evident. These folds, which will also be refered to as F_3, generally have larger amplitudes than kink folds. The uniform orientation of the crenulation foliation S_2 (Figure 6) indicates that F_3, which deformed this structure, does not form large folds within the area mapped.

Small folds, designated as F_4, developed by slippage on S_3 (Plate 12). These folds, which have axial planes parallel to S_3 and fold axes normal to L_3, are rarely evident.

Fractures

Fractures are ubiquitous within the area mapped. One set is vertical and strikes northwest. A second set dips steeply to the southwest. Both sets are weakly developed. A third well-developed set is characterized by tension fractures.

Vertical tension fractures strike from northwest to northeast but as synoptically shown in Figure 9, they have two prefered orientations and form a conjugate set. Conjugate tension fractures are present within some outcrops although most contain only one set. Tension fractures typically are discontinuous and occur en echelon. Their width is 0.1 mm to greater than 3 mm with lengths of 1 mm to more than 5 meters. Tension fractures commonly are filled with chlorite and/or suphides.

Tension fractures appear to have developed as late structures during the same deformation which produced the conjugate wrinkle lineations, L_2 and conjugate kink and open folds, F_3. The following observations support these

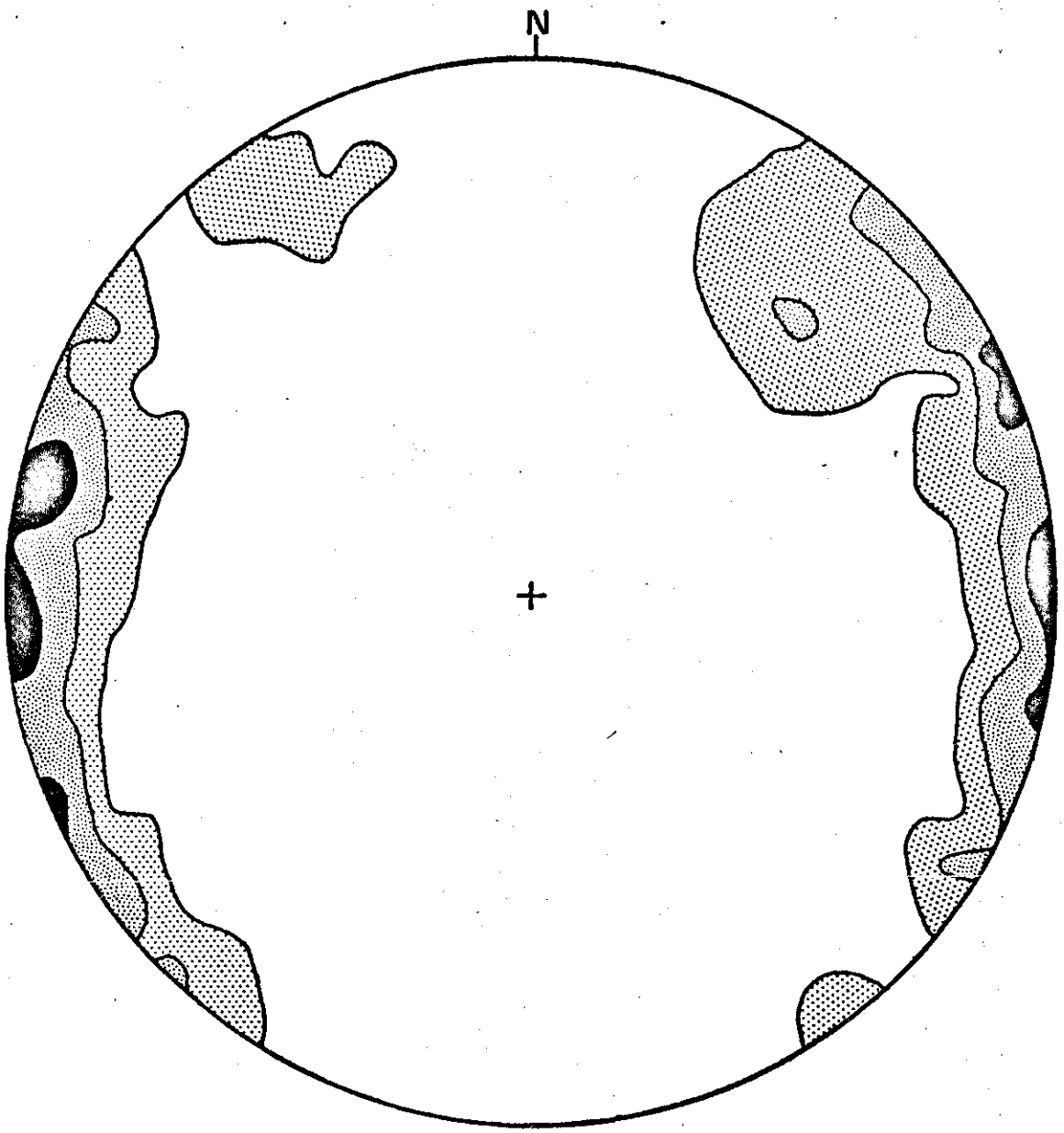

PER ONE PERCENT AREA

1 – 5%

5 – 10%

>10%

Fig 9. Plot of poles to fractures (122 plotted).

inches
0 1
0 1 2
centimetres
This reference scale bar has been added to the original image. It will scale at the same rate as the image, therefore it can be used as a reference for the original size.

conclusions:

1. A line drawn on Figure 9 which would bisect the angle between the conjugate set of tension fracture (approximately north 10 degrees west) would also bisect L_2 (Figure 7) and F_3 (Figure 8).

2. Some tension fractures show displacements along planes parallel to the crenulation foliation, S_2.

3. Most tension fractures transect L_2 and F_3 without deflection.

The first observation suggests that the tension fractures, L_2 and F_3 developed during the same deformation. The second observation suggests that the development of tension fractures was in part synchronous with the formation of L_2 and F_3 (renewed slippage along S_2 accompanied the formation of L_2 and F_3). That most tension fractures developed after L_2 and F_3 is implicit in the third observation.

Large-Scale Structures

Large-scale structures, notable folds, are not apparent in the field but probably do occur. One such structure, near the center of the map-area, is indicated by the sudden flexure of copper-bearing horizons. However, the geometry of this flexure is best displayed by the faulted lens of quartzite just below the Noranda camp (Figure 4). When reconstructed, this quartzite lens is S-shaped and has the same geometry and orientation as the small-scale gleitbret folds developed between S_2 planes. A similar large structure can be infered from the distribution of Unit 5 lithologies in the southern part of the map-area. These lithologies may outline the northern half of a subisoclinal fold which has been transposed into irregular-shaped lenses. Small-scale subisoclinal folds have the same orientation as this structure and display a similar style of transposition.

Andesite Dykes

The margins of altered andesite dykes locally are sheared and brecciated.

Internally, the dykes are relatively undeformed. Slickensided surfaces, of the same appearance as S_3, locally are developed.

Chlorite-Biotite Gneiss

Alignment of biotite and/or chlorite imparts a good foliation to the rocks of Unit 11. This foliation parallels S_2 in the overlying phyllites and is the only important structure developed. The foliation S_3 and lineation L_3 are weakly developed but folds and tension fractures are notably absent.

Interpretation

The keys to the structural history of the map-area are small-scale structures within the Eagle Bay Formation. These rocks exhibit the effects of four periods of deformation which are in general agreement with the deformational history described by Campbell and Okulitch (1973) for the Mount Ida Group and Fyson's (1970) model of deformation for rocks in the Shuswap Lake Area, British Columbia. Earliest recognizable deformation produced a foliation parallel to subparallel to bedding. This structure does not appear to be related to macro- or mesoscopic folds but seems "to have been produced by some mechanism akin to intrafolial flow" (Campbell and Okulitch, 1973). The second period of deformation is characterized by intense shearing with the development of a penetrative crenulation foliation, gleitbrett folds and subisoclinal folds. Conjugate sets of folds, wrinkle lineations and tension fractures were formed during the third period of deformation. The fourth, and youngest period of deformation, is characterized by weak, nonpenetrative shearing with the development of slickensided surfaces and small slip-folds. Structural features of the Eagle Bay Formation within the area mapped are summarized in Table IV.

Deformation Period	Structure	Description	Relative Direction of Movement
I	S_1	Earliest recognizable foliation: parallel to subparallel to bedding.	
II	S_2	Crenulation foliation; transposes bedding and earlier foliation S_1.	
	L_1	Intersection of S_2 with bedding or S_1; crests of minute gleitbret folds.	
	F_1	Subisoclinal folds with fold axes = L_1; most commonly reclined with axial planes = S_2; display transposition along S_2.	
	F_2	Gleitbret folds; S-shaped with axial planes = S_2 and fold axes = L_1	East to west
III	L_2	Northwest- and northeast-plunging wrinkle lineations.	Northerly
	F_3	Conjugate sets of kink and open folds; co-axial with L_3.	Northerly
	Tension Fractures	Average north-south orientation; vertical and form a conjugate set.	
IV	S_3	Slickensided surfaces.	
	L_3	Slickensides on S_3.	Northwest
	F_4	Slip folds with fold axes normal to L_3 and axial planes parallel to S_3.	

Table IV Structural Features of the Eagle Bay Formation, Harper Creek

Emplacement of andesite dykes (Unit 9) post-dates the second period of deformation but appears to pre-date the fourth period of deformation. The dykes probably were intruded into tensional structures during or following the third period of deformation. As previously noted, an andesite dyke south of the map-area has a vertical orientation with a northerly strike. This attitude closely approximates the average attitude of tension fractures developed during the third period of deformation.

The foliation in the chlorite-biotite gneiss probably was developed by weak, but penetrative, plastic shear during the first and/or second period of deformation. Notably absent from the gneiss are the subisoclinal and gleitbret folds which developed within rocks of the Eagle Bay Formation during the second period of deformation. Their absence may be explained by a difference in rock competency. Unit 10, an homogeneous lithology, possibly acted as a competent mass which did not yield to deformation as readily as the overlying incompetent, heterogenous mixture of metavolcanic and metasedimentary rocks representative of the Eagle Bay Formation. Within the map-area, the third period of deformation is not recorded in the rocks of Unit 10. However, Unit 10 does appear to form the core of a major antiform south of the map-area which may have formed during this deformation. The axial orientation of this fold is east-west, normal to the maximum compression direction for the third period of deformation. The map-area is situated on the north limb of this fold.

Ages of Deformation

Descriptions given by Campbell and Okulitch (1973) indicate that the Mount Ida Group (includes the Eagle Bay Formation) displays structures which characterize the first three periods of deformation within the area mapped by the writer. Campbell and Okulitch suggest a lower age limit of Upper Triassic

for the deformation(s) which produced these structures. This conclusion appears to be based, for the most part, on the correlation of an Upper Karnian or Lower Norian conodont-bearing limestone unit with the Sicamous Formation of the Mount Ida Group.

A simplified sketch of the Thuya, Raft and Baldy batholiths as shown in Figure 10 illustrates a close correlation between the orientation of these batholiths and large east-west trending folds which are thought to have formed during the third period of deformation. The Baldy batholith occupies the axial region of one of these folds but its emplacement appears to post-date the formation of the fold. The implication is that the emplacement of the Baldy batholith was strongly controlled by this pre-existing structure. A similar structural control is suggested for the emplacement of the Raft and Thuya batholiths. If correct, this implies that the upper age limit for the third period of deformation is Lower Jurassic-Upper Triassic (the oldest potassium-argon age for the Thuya batholith is 198 m.y.).

The plot of modal data for the Thuya, Raft and Baldy batholiths is shown in Figure 3 and illustrates a corresponding compositional difference and degree of differentiation with age. Younger rocks trend towards an enrichment in quartz and potassium feldspar relative to plagioclase and are more variable in composition. The data appear to define a straight-line differentiation series which originates from the quartz diorite end of the field. The writer believes that the dykes of Unit 9 occupy tensional features developed during the third period of deformation and that the composition of the dykes would plot close to the bottom of this trend. Because of this apparent compositional similarity and because of the apparent relation of intrusive rocks in the area to structures developed during the third period

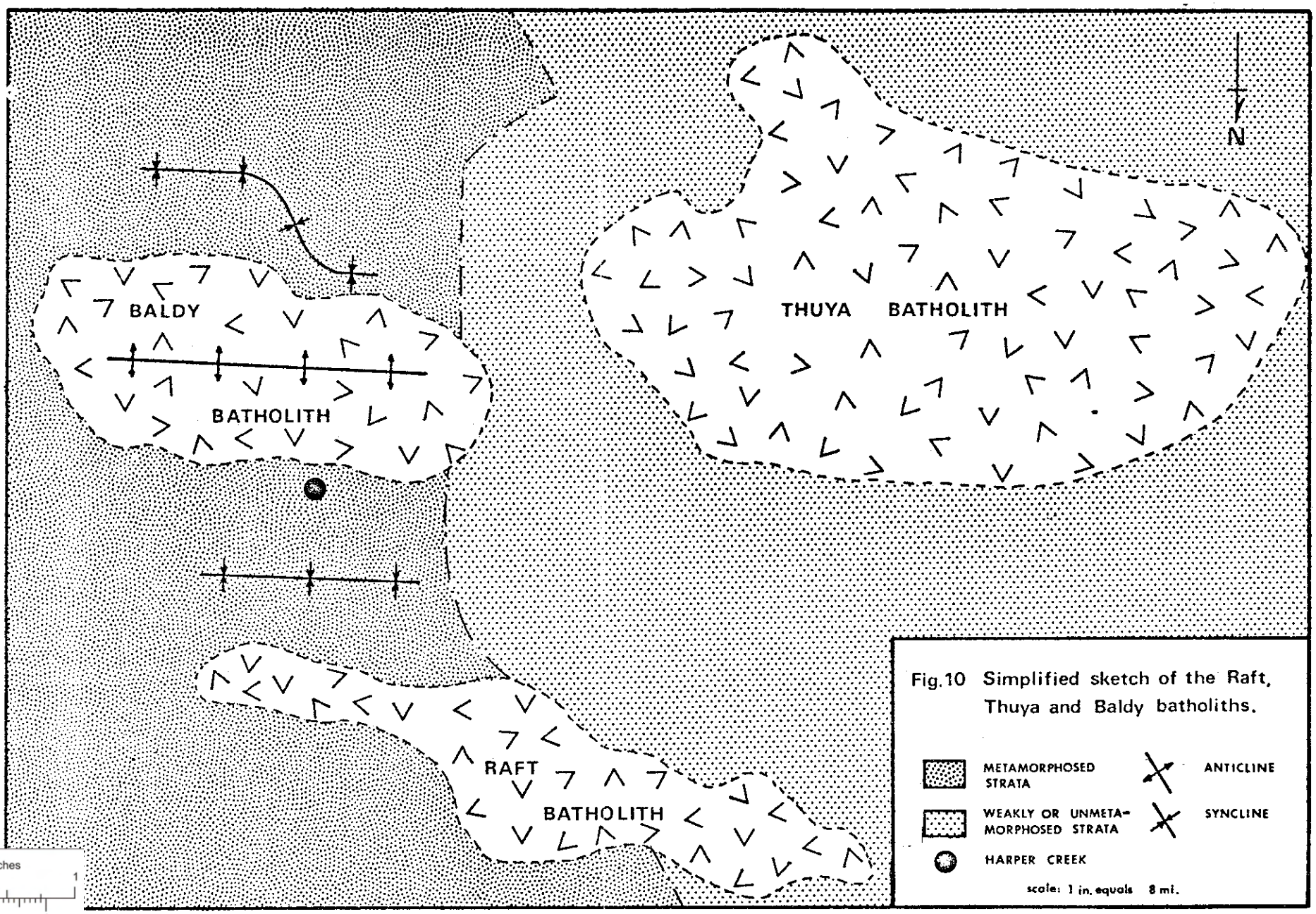

Fig.10 Simplified sketch of the Raft, Thuya and Baldy batholiths.

inches
0 1
0 1 2
centimetres
This reference scale bar has been added to the original image. It will scale at the same rate as the image, therefore it can be used as a reference for the original size.

of deformation the writer believes the dykes are part of a differentiational series and are as old or older than the rocks of the Thuya batholith. If correct, this supports an upper age limit for the third period of deformation of Lower Jurrassic-Upper Triassic.

Although tenuous, evidence presented above indicate that the first three periods of deformation occurred between Upper Triassic (Upper Karnian or Lower Norian) and Lower Jurassic-Upper Triassic. The age of the fourth period of deformation is unknown but possibly is related to the intrusion of the Early Upper Cretaceous Baldy batholith.

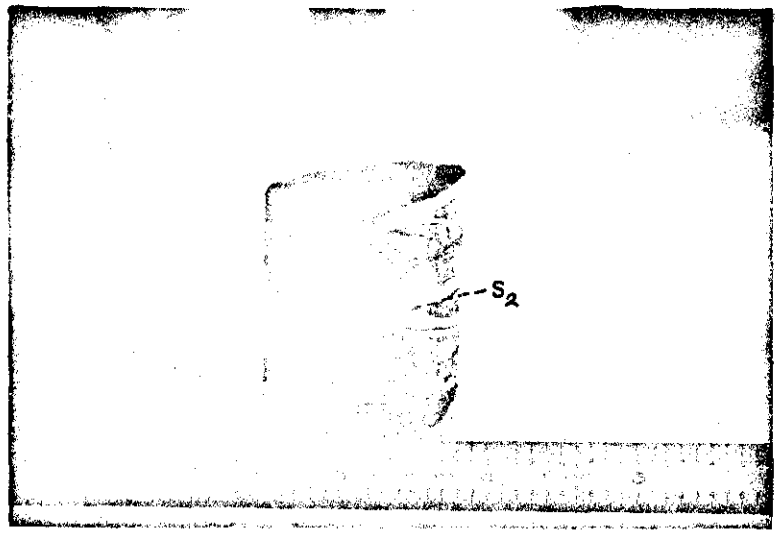

Plate 9 Photograph of sandy graphitic phyllite from Unit 5 illustrating relation between bedding (alternating dark and light laminations) and S_2. Note that bedding has been folded into F_1 prior to being transposed along S_2. Also note gleitbret folds (F_2) developed between S_2 planes. Scale is in inches.

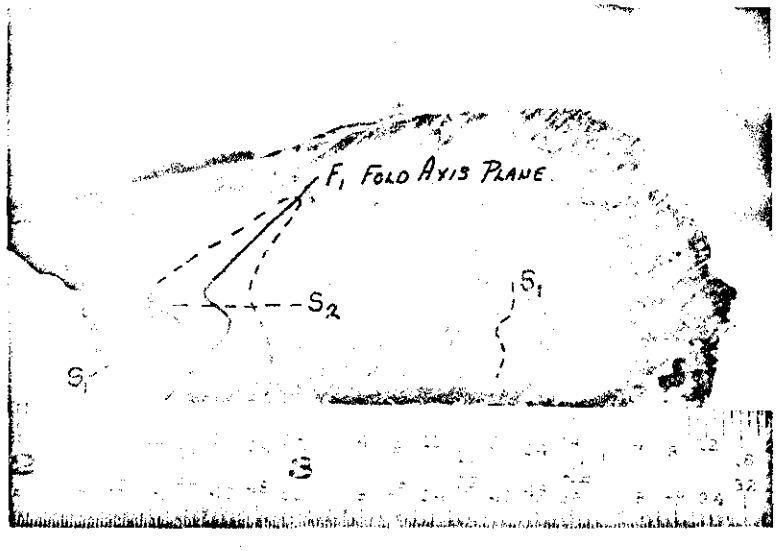

Plate 10 Photograph showing early foliation (S_1) folded into upright subisoclinal fold (F_1). Note partial transposition of F_1 along S_2. Scale is in inches.

1 mm 0 mm
scale

Plate 11 Photomicrograph of sandy graphitic phyllite from Unit 5, plain polarized light. Photograph shows bedding (alternating dark and light lamination) folded into a subisoclinal structure (F_1). An early foliation (S_1) is developed parallel to bedding. Also evident are small, S-shaped, gleitbret folds (F_2) developed between S_2 planes.

1 mm 0 mm
scale

Plate 12 Photomicrograph showing late slip folds (F_4). Folds developed by drag along slickensided surfaces (S_3).

Chapter V

MINERAL DEPOSITS

Within the map-area, mineralization is widespread and characterized by a wide variety of sulphides, silicates, oxides and carbonates (listed in approximate order of decreasing abundance in Table V). Pyrite, the most abundant sulphide, is found in all rock types. Copper sulphides, notably chalcopyrite, are the only minerals of economic importance and occur almost exclusively within rocks of the Eagle Bay Formation (Units 1 to 9).

PRIMARY	SECONDARY
<u>Metallic</u>	limonite
	hematite
pyrite	manganese oxides
pyrrhotite	jarosite
chalcopyrite	malachite
sphalerite	covellite
arsenopyrite	azurite
molybdenite	hydrozincite
galena	melanterite
tetrahedrite-tennantite	native copper
bornite	cuprite
cubanite	chalcocite
	chrysocolla
<u>Non-metallic or Submetallic</u>	tenorite ?
	anglesite
chlorite	
dolomite	
sphene	
magnetite	
quartz	
albite	
sericite	
tourmaline	
magnesite	
rutile	
biotite	

Table V Primary and Secondary Minerals in the Harper Creek Area.

Iron oxides, the most abundant secondary minerals, have formed to depths in excess of 200 feet. Secondary copper minerals generally are restricted to near-surface exposures.

Mineralization

The main period of mineralization within the Eagle Bay Formation appears to have been, in part, synchronous with the third deformational period. Sparsely mineralized quartz, carbonate and quartz-carbonate veins were developed during a second period of mineralization.

Main Period

The main period of mineralization developed in two stages. The first and economically most important stage (Stage I) was largely synchronous with, but also preceded, folding of the third period of deformation. During deformation earlier-formed sulphides were being deformed and recrystallized as new sulphides precipitated. The development of tension fractures, a late phase of the third period of deformation, marked the beginning of the second stage of mineralization (Stage II).

Sulphides

Sulphides deposited during Stage I mineralization are, in order of decreasing abundance: pyrite, pyrrhotite, chlacopyrite, sphalerite, arsenopyrite, molybdenite and cubanite. Pyrite, pyrrhotite and chalcopyrite together comprise more than 99 percent of the total sulphide. The pyrite: pyrrhotite ratio is estimated at 5:1 and the pyrrhotite:chalcopyrite ratio is about 3:1. Sphalerite, although widespread, rarely exceeds 1 percent. Arsenopyrite, molybdenite and cubanite are only locally evident.

Chalcopyrite and minor pyrite were the only sulphides deposited during Stage II mineralization. The ratio of Stage I chalcopyrite:Stage II chalcopyrite is approximately 10:1.

Stage		Occurrence	Sulphide(s)
I	1)	evenly disseminated	py, cpy, po, sph, arsenopyrite
	2)	bands of disseminated sulphide	py, cpy
	3)	thin sulphide bands	py, cpy
	4)	smears along foliation planes	cpy, po, mo, py
	5)	irregular veins and patches	py, cpy
	6)	in thin conformable quartz and quartz-carbonate veins	py, cpy
	7)	massive sulphide lenses	py, po, cpy
	8)	replacements of pyrite	po, cpy
	9)	coating sphene grains	py, cpy
	10)	partial to complete replacement of carbonate porphyroblasts	py, cpy
	11)	inclusions within other sulphides	sph, cub
II	12)	coating tension fractures	cpy, minor py
	13)	vein fillings	cpy, minor py
	14)	disseminations away from mineralized veins or fractures	cpy, minor py

Table VI Sulphide Deposition During the Main Period of Mineralization, Harper Creek.

Modes of occurrence for sulphides deposited during the main period of mineralization are summarized in Table VI. Replacement textures characterize sulphides deposited during Stage I mineralization and planar structures defined by sulphide concentrations generally parallel the crenulation

foliation, S_2. Stage II sulphides occur as vein and fracture fillings and as disseminations adjacent to mineralized veins and fractures.

Stage I

Most pyrite and chalcopyrite deposited during Stage I mineralization occur evenly disseminated over large areas. Although chalcopyrite generally is associated with pyrite, pyrite without chalcopyrite is commonly observed. Pyrite content does not exceed 10 percent. Chalcopyrite content rarely exceeds 2 percent. Most pyrite is fine to medium grained and euhedral. Fine-grained, anhedral chalcopyrite occurs interstitially.

Other sulphides which occur evenly disseminated are sphalerite, pyrrhotite and arsenopyrite. Sphalerite, which does not exceed 1 percent, is fine-grained, brown and resinous. Fine-grained pyrrhotite generally is associated with chalcopyrite. Arsenopyrite, which is only locally evident, is fine to medium grained and euhedral.

Bands of disseminated sulphides, in which the pyrite content exceeds 10 percent and chalcopyrite may exceed 4 percent, occur sporadically within the disseminated sulphide zones. Pyrite-rich bands are less than 5 mm to more than 30 feet in thickness. Chalcopyrite-rich bands seldom exceed a thickness of more than 10 feet. Although somewhat coarser grained, sulphide textures are the same as in the evenly disseminated zones.

Laminations of pyrite and/or chalcopyrite occur within disseminated sulphide zones but are more common within bands of concentrated sulphide. Sulphide laminations are 1 cm or less in thickness and parallel the crenulation foliation, S_2. Some have been traced along strike for more than 20 feet.

Some sulphides are smeared on S_2. These smears cover areas up to several square cm and are a few microns to 1 mm thick. Pyrrhotite, chalcopyrite and molybdenite smears occassionally attain a mirror-like polish. Pyrite smears are far less lustrous and often are difficult to see. Shear between S_2 planes, which accompanied folding as flexture slip during the third period of deformation appear to have caused development of smeared sulphides. The presence of undeformed sulphides on smear surfaces indicates sulphide deposition continued after folding.

Within the quartzites of Unit 6, chalcopyrite and pyrite commonly fill irregular veins and patches. Drusy cavities, characteristic of open space fillings locally are evident.

Within the phyllites of Unit 4, pyrite and chalcopyrite occur in thin quartz and quartz-carbonate laminations. Laminations are but a few mm thick and parallel S_2. Laminations pre-date mineralization and are common in nonmineralized rock.

Lenses of massive sulphide were noted at a few locations. These lenses range from less than 5 feet to greater than 30 feet in thickness and have sharp or gradational contacts with the enclosing host rocks. The principal sulphides are fine- to coarse-grained pyrrhotite and pyrite, with local concentrations of chalcopyrite.

Most pyrrhotite occurs as partial to complete replacements of pyrite in rocks above the main copper-bearing horizon. Cubic pseudomorphs are common and many pyrrhotite pseudomorphs have pyrite cores. Polished smears of pyrrhotite, which appear to be deformed pyrrhotite pseudomorphs of pyrite,

indicate alteration of pyrite to pyrrhotite occurred early in the first stage of mineralization. At a few localities, pyrite and/or cubic pseudomorphs of pyrrhotite have been partly replaced by chalcopyrite.

Sulphides developed during the first stage of mineralization also include: 1) pyrite and chalcopyrite coating fine-grained sphene, 2) pyrite and/or chalcopyrite partly to completely replacing carbonate porphyroblasts (Plate 13) and 3) minor sphalerite and cubanite as small inclusions in chalcopyrite.

Stage II

Most chalcopyrite deposited during Stage II mineralization occurs in tension fractures. Tension fracture density varies from less than 1 to more than 10 per square foot but generally less than 10 percent contain chalcopyrite. Generally, the number of tension fractures mineralized with chalcopyrite increases towards copper-bearing horizons. Tension fractures which display offsets along planes parallel to S_2 are thought to have developed during folding as offsets appear to be the result of flexure slip.

Chalcopyrite also occurs within veins which generally consist of three or more of the following: dolomite, chlorite, tourmaline, albite, quartz and minor rutile. Gangue minerals locally are zonally arranged parallel to vein walls (Plate 14).

Disseminations of chalcopyrite and minor pyrite adjacent to mineralized veins and fractures are common. Narrow sulphide halos around tension fractures are confined to the immediate vicinity of the fracture. Sulphide halos around veins are more extensive and occur as irregular disseminations

and as laminations of disseminated sulphide which parallel S_2.

Silicates, Oxides and Carbonates

Silicates, oxides and carbonates deposited during the main period of mineralization include: carbonate, albite, quartz, sphene, chlorite, magnetite, tourmaline and rutile. Carbonate, albite and quartz are vein constituents but also occur as porphyroblasts disseminated within sulphide zones and as disseminations adjacent to mineralized veins and fractures. Poryphyroblasts, which are subhedral to euhedral, are 0.5 mm to 4 mm across. Carbonate porphyroblasts are most abundant and often display twinning indicative of dolomite. Albite porphyroblasts were observed only adjacent to mineralized veins.

Some sphene, probably of hydrothermal origin, was observed as replacements of phyllite adjacent to mineralized veins (Plate 14). Sphene, previously noted as occurring as partial to complete replacements of carbonate porphyroblasts and carbonate within the matrix of some phyllites, is also thought to be of hydrothermal origin.

Chlorite occurs within veins and coating tension fractures. In thin section, between cross nicols, this chlorite displays an anomalous berlin blue interference color suggestive of penninite. Although tension fractures mineralized with chalcopyrite almost always contain chlorite the converse is not true.

Massive magnetite occurs within sulphide lenses and as separate lenses and layers. Magnetite is coarse grained and contains variable amounts of chlorite and chalcopyrite.

Dark green to brown tourmaline occurs as vein fillings and as replacements around tourmaline-bearing veins. Rutile, which locally displays elbow twinning, occurs as an accessory mineral in veins.

Alteration

Alteration of host rocks during the main period of mineralization involved an early recrystallization of sericite and chlorite formed by regional metamorphism and a later chloritization. Recrystallized micas are petrographically distinguished from the crenulation foliation S_2 by the synchronous extinction of micas and by a difference in optical properties of chlorite. Chlorite formed by regional metamorphism is light to medium green and displays a light to dark grey birefringence (possibly prochlorite) whereas recrystallized chlorite is generally a darker green and displays an anomalous blue birefringence (possibly penninite).

The distribution of zones of recrystallized mica is not precisely known but there appears to be a close spatial relation to areas of sulphide mineralization. The age of recrystallization appears to largely predate the third period of deformation.

Formation of secondary chlorite as an alteration of sericite was closely related to sulphide deposition. This chlorite, which optically also has the appearance of penninite, occurs as zones of complete replacement, irregular patches, fine disseminations and as envelopes adjacent to mineralized veins and fractures.

Completely chloritized phyllite of Unit 4 is difficult to distinguish from the chlorite-rich rocks of Unit 8, and because of this, some rocks which were mapped in the field as part of Unit 8 were later suspected as

representing chloritized rocks of Unit 4. From what is known, completely chloritized rocks occur as small lenses and pods within mineralized horizons and their inclusion as part of Unit 8 does not appreciably affect the distribution of Unit 8 lithologies as mapped. Petrographically, distinction between completely chloritized rocks and Unit 8 rocks is based upon the amount of sphene present. Sphene, a major constituent of Unit 8, generally forms a minor part of chloritized rocks.

Secondary chlorite also occurs as small, irregular patches and as fine disseminations within and adjacent to areas of sulphide mineralization. Where chlorite is finely disseminated, the rocks have a spotted green appearance (Plate 15).

Secondary chlorite is closely associated with mineralized veins and fractures and occurs as halos, laminations and disseminations adjacent to vein and fracture walls (Plate 16). Chlorite halos are less than ½ inch to more than 2 inches wide. Chlorite laminations, which parallel the foliation S_2, normally are less than ¼ inch thick. Some chlorite disseminations have sulphide or albite cores (Plate 16).

Paragenesis

The sequence of deposition of primary minerals during the main period of mineralization is shown in Figure 11. On the basis of textures, cross-cutting relationships and relative timing with the third period of deformation this sequence was as follows:

oldest
carbonate
sphene
pyrite
chlorite
molybdenite
arsenopyrite
magnetite
pyrrhotite

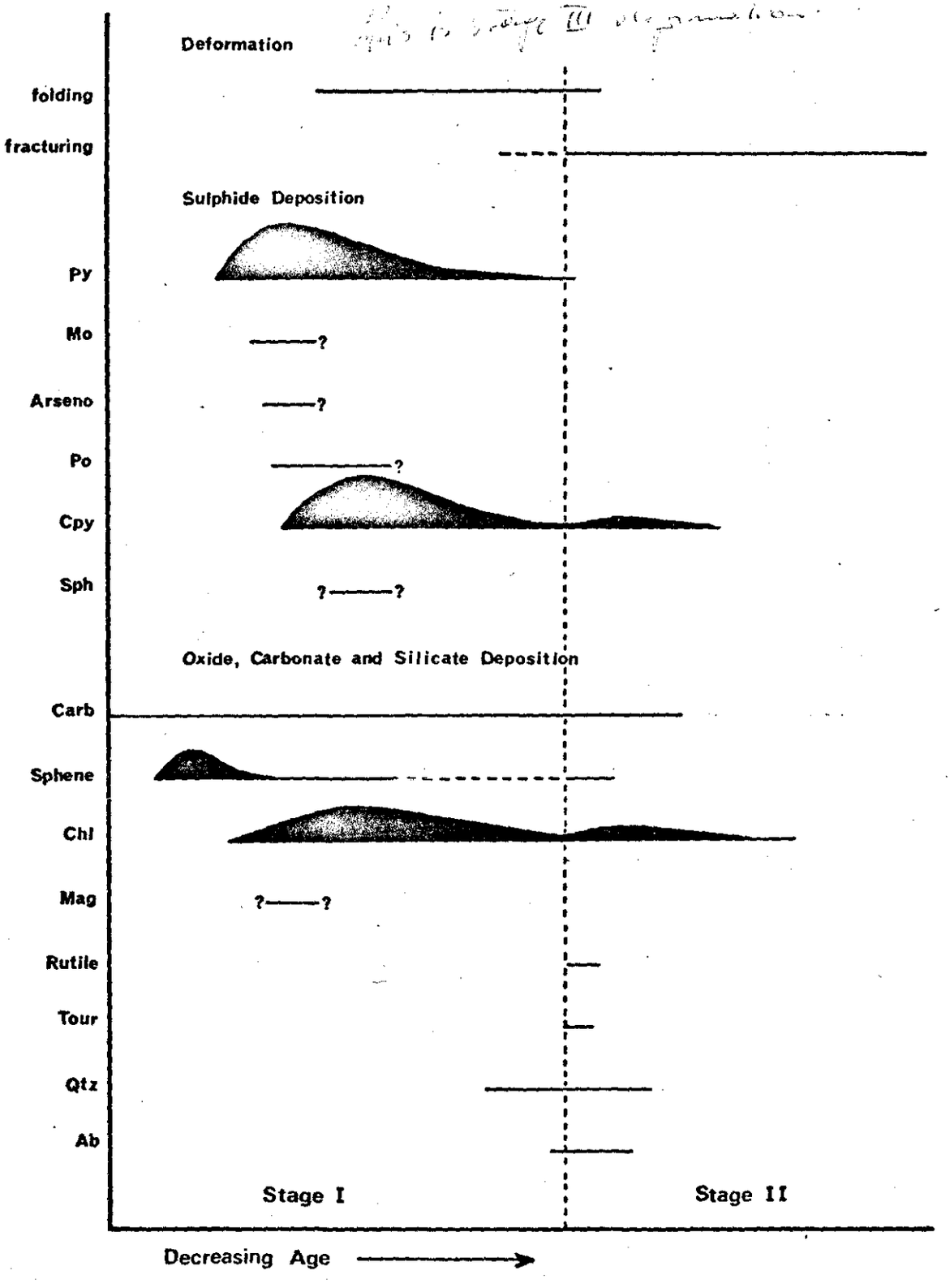

Fig 11. Sequence of deposition of primary minerals during the main period of mineralization.

chalcopyrite
sphalerite
quartz
albite
tourmaline
youngest rutile

Field relations suggest mineralization was continuous with the bulk of mineralization occurring before the large-scale development of tension fractures. Nonmineralized tension fractures adjacent to mineralized tension fractures suggest fracturing outlasted mineralization.

Form of the Deposits

Areas with greater than 0.2 weight percent copper over true thicknesses exceeding 50 feet are outlined on Figure 4 and are shown on Sections II, V and VI. The 0.2 weight percent cut-off serves as a natural demarcation because values outside these areas generally are an order of magnitude lower. Copper values within these areas are uniform and rarely exceed 1 weight percent over a true thickness exceeding 10 feet.

Copper mineralization is confined to tabular-shaped bodies which have an average east-west strike and a fairly uniform northerly dip. The Main Mineralized Horizon (Figure 4) has a continuous strike length of more than 6000 feet and a true thickness of up to 400 feet. This zone has been explored along its dip length for 2000 feet. More than 90 percent of the copper within these horizons was deposited during Stage I mineralization. Most of the remainder was deposited during Stage II.

Structural Controls

The crenulation foliation S_2 was locally important for the channeling of 'ore-forming' fluids but does not appear to be responsible for the overall distribution of copper-bearing horizons. Large-scale structures appear to have had an important role. One such structure is the S-shaped fold located

near the center of the map-area and is illustrated in Figure 12, which is a structure-contour map of the footwall of the main mineralized horizon. Copper mineralization does not appear to be deformed by this structure but rather appears to fan-out from this centrally located structure.

The southern part of the main mineralized horizon east of the central flexure dips steeply (60 to 90 degrees) to the north and rapidly flattens towards the north to a more uniform dip of about 30 degrees north (refer to Figure 12 and Sections V and VI). This structure resembles the lower half of an isoclinal fold with an east-west axis orientation. The geometry of this structure is anomalous and does not correlate with any previously discussed structures. Possibly there is a relationship with the early foliation S_1.

Stratigraphic Controls

Copper mineralization does not appear to be stratigraphically controlled. The overall pattern of mineralization is one of transgression. Surface traces of copper-bearing horizons have an average east-west orientation. Stratigraphic units have a prefered northeast-southwest orientation. Although copper-bearing horizons usually conform with stratigraphy down-dip (Sections V and VI) there are marked discordancies (Section II).

Although copper-bearing horizons do not appear to be stratigraphically controlled, stratigraphy was important in the locallization of higher grade zones. Unit 8 lithologies, notably chlorite phyllite, appear to be the best hosts for copper mineralization. This relationship is graphically illustrated in Figure 13. Titanium values, which also are graphically shown in Figure 13, illustrate a close correlation with lithologies. One exception

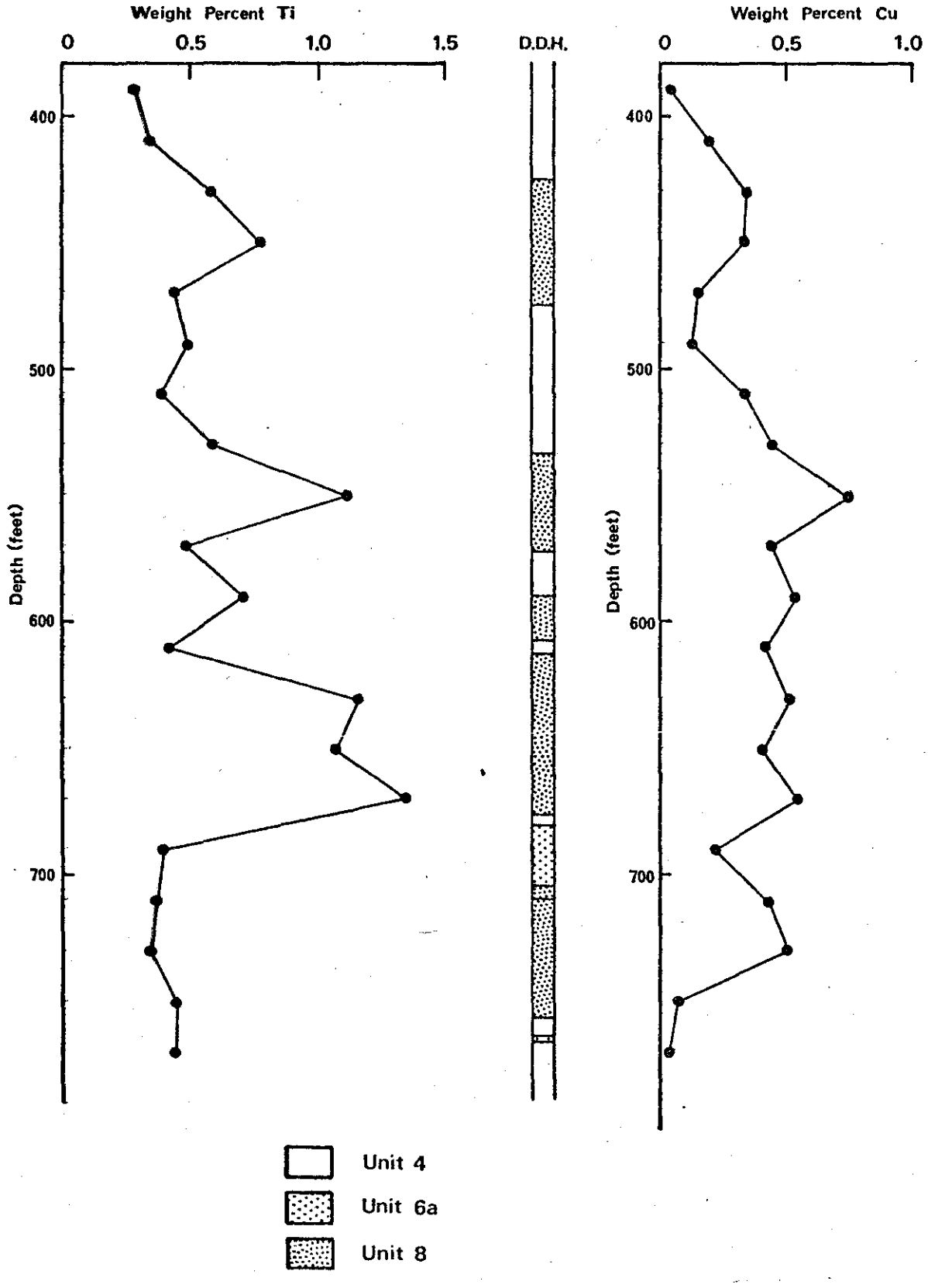

Fig 13 Graphical plot of a diamond-drill hole log (D.D.H) with corresponding titanium and copper values.

inches
0
1
0
1
2
centimetres
This reference scale bar has been added to the original image. It will scale at the same rate as the image, therefore it can be used as a reference for the original size.

occurs near the bottom of the diamond-drill hole in a chloritic quartzite member which would probably have lower primary titanium values. Also evident is a correlation of higher titanium values within members of Unit 8 with higher copper values.

Second Period

Sulphides deposited during the second period of mineralization are, in approximate order of decreasing abundance: pyrite, chalcopyrite, pyrrhotite, sphalerite, galena, tetrahedrite-tennantite and bornite. These fine- to coarse-grained sulphides occur as disseminations and patches within quartz, carbonate and quartz-carbonate veins. The veins are ½ inch to more than 1 foot in width and cut structures developed during the third period of deformation. Vein walls locally are silicified with local development of bright green hydrothermal sericite. Most vein carbonate is dolomite although magnesite and calcite also were identified by X-ray techniques.

Sulphur Isotopes

Sulphur isotope data for sulphide samples collected within the present area of study is made available in an unpublished Master of Science thesis entitled "Sulfide Deposition at Noranda Creek, B.C." by K.J. Kirkland (1971). The values obtained for pyrite and chalcopyrite appear in Figure 14. All values are given as δS^{34} (per mil) where:

$$\delta S^{34}(‰) = \frac{S^{34}/S^{32}(\text{sample}) - S^{34}/S^{32}(\text{standard})}{S^{34}/S^{32}(\text{standard})} \times 1000$$

$\delta S^{34} = 0.00‰$ for troilite from the Cañon Diablo meteorite was used as a standard.

Kirkland has interpreted the data as representing one period of mineralization. From Figure 14 it appears possible that there are two δS^{34} populations. The sulphur isotope analyses for chalcopyrite and pyrite from mineralized veins fall with the range of - 5‰ to + 5‰. Kirkland's description of veins resembles veins from the second period of mineralization but he does not describe veins similar to those developed during the first period of mineralization. Disseminated chalcopyrite as well as pyrite and chalcopyrite from tension fractures fall within the range of + 1‰ to + 9‰. Diffusion mechanisms cannot explain these differences. In his thesis, Kirkland states:

> "The mechanism of isotopic diffusion would produce 'light' wall rock sulfides and relatively 'heavy' vein sulfides. This pattern is the reverse of the pattern found at Noranda Creek so the diffusion mechanism is not believed responsible for the overall sulfur isotope pattern found within the thesis area."

A possible alternative to Kirkland's interpretation is that vein sulphides had a different source of sulphur than disseminated sulphides or sulphides found in tension fractures. Kirkland has demonstrated that δS^{34} values for vein sulphides appear to be zonally arranged with values decreasing towards the Baldy batholith. Such zoning is not apparent for disseminated sulphides or sulphides found in tension fractures.

Genesis

The following field relations help support a hydrothermal origin for the main period of mineralization at Harper Creek:

1) It appears that the main period of mineralization was synchronous with the third period of deformation.

2) Although stratigraphy is important for the localization of higher grade mineralization, the overall pattern is one of transgression.

3) Stratigraphic units typically are discontinuous, whereas mineralized horizons display continuity (the main copper-bearing horizon

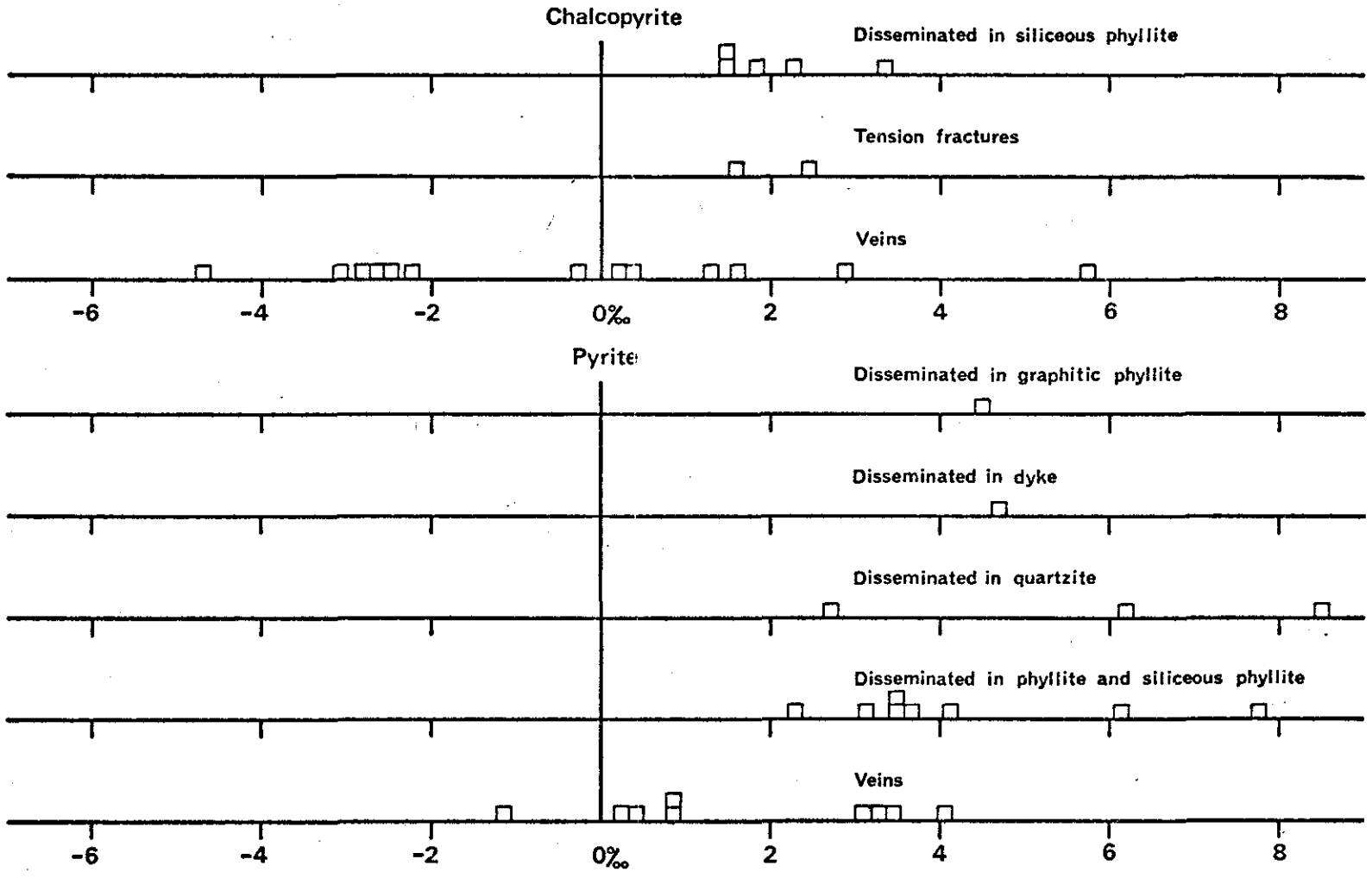

Fig 14 δS^{34} values for pyrite and chalcopyrite; data from Kirkland, 1971, pp. 27-29.

has a continuous strike length of over 6000 feet).

4) Most sulphides display replacement textures.

5) Mineralization appears to post-date regional metamorphism thereby weakening arguments for remobilized syngenetic sulphide.

6) Sulphides deformed prior to the third period of deformation were not observed.

7) Sulphides conforming to small-scale folds developed prior to the third period of deformation were not observed.

The main period of mineralization at Harper Creek does not appear to be genetically related to known intrusives within the area. The Baldy batholith is thought to post-date the deposit and there is no apparent relationship between mineralization and andesite dykes (Unit 9).

An alternative hypothesis is that mineralizing fluids are of hydrothermal metamorphic origin. The regional distribution of 'Harper Creek-type' occurrences, as shown in Figure 15, lends support to this idea. All 'Harper Creek-type' occurrences are located on the limbs of an east-west oriented antiform (core of antiform occupied by the Baldy batholith) and occur near the contact between chlorite-biotite gneiss and rocks of the Eagle Bay Formation (ie, near the biotite isograd). Formation of the antiform is thought to have occurred during the third period of deformation and therefore is synchronous with the main period of mineralization at Harper Creek. The following model is suggested to account for the observed nature of the Harper Creek copper deposit and for the distribution of 'Harper Creek-type' occurrences:

> 'Harper Creek-type' occurrences are genetically related to the formation of the large east-west oriented antiform situated south of the map-area. The deposits were formed by mineralizing fluids of hydrothermal metamorphic origin which migrated into this structure and replaced favorable host rocks.

The model presented to explain the biotite-actinolite zone in rocks

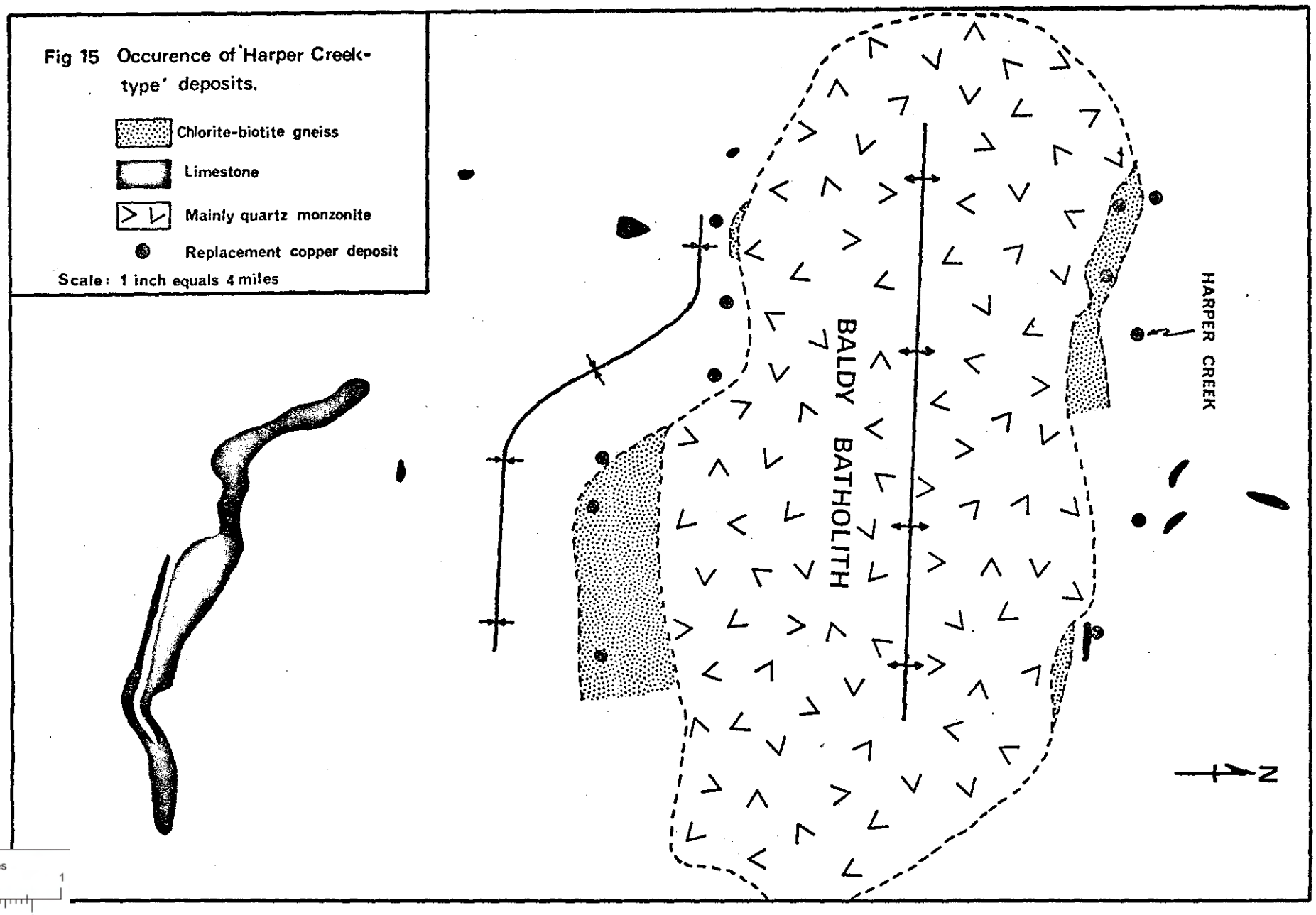

Fig 15 Occurence of 'Harper Creek-type' deposits.

inches
0 1
0 1 2
centimetres
This reference scale bar has been added to the original image. It will scale at the same rate as the image, therefore it can be used as a reference for the original size.

adjacent to the gneiss is consistent with this hypothesis. In this model it was suggested that the gneiss, which was still undergoing metamorphism, was folded and squeezed into cooler overlying strata resulting in the raising of isotherms with the partial readjustment of the contact rocks to the new temperature conditions. If this event occurred during formation of the antiform it would support an hypothesis of hydrothermal metamorphic fluids rising into this structure.

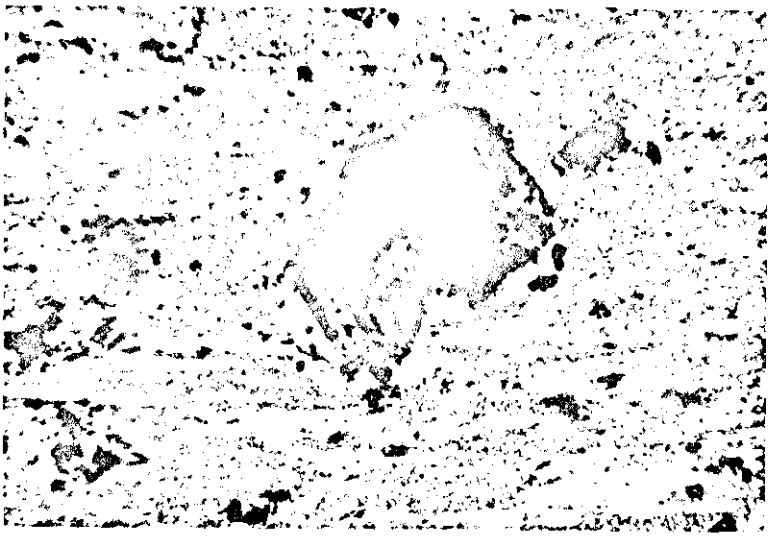

1 mm 0 mm

scale

Plate 13 Photomicrograph showing sulphide (opaque mineral) occurring as replacements of carbonate porphyroblasts (center of photograph), plain polarized light.

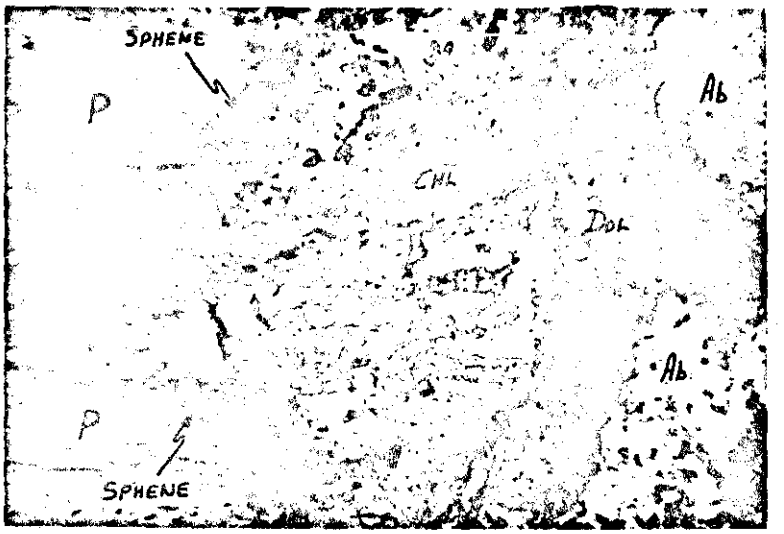

1 mm 0 mm

scale

Plate 14 Photomicrograph of part of a Stage II vein, plain polarized light. Note that gangue minerals, which include dolomite (Dol), tourmaline (T) and chlorite (Chl), are zonally arranged parallel to the vein wall. Also note that sphene (opaque mineral) appears to have replaced phyllite (P).

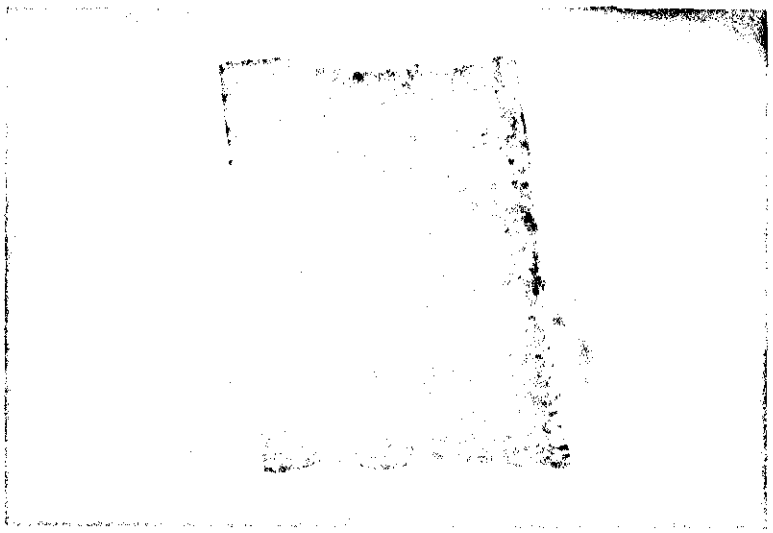

Plate 15 Photograph illustrating chlorite alteration (dark specks) which imparts a speckeled appearance to some of the rocks. Width of specimen is about 1¼ inches.

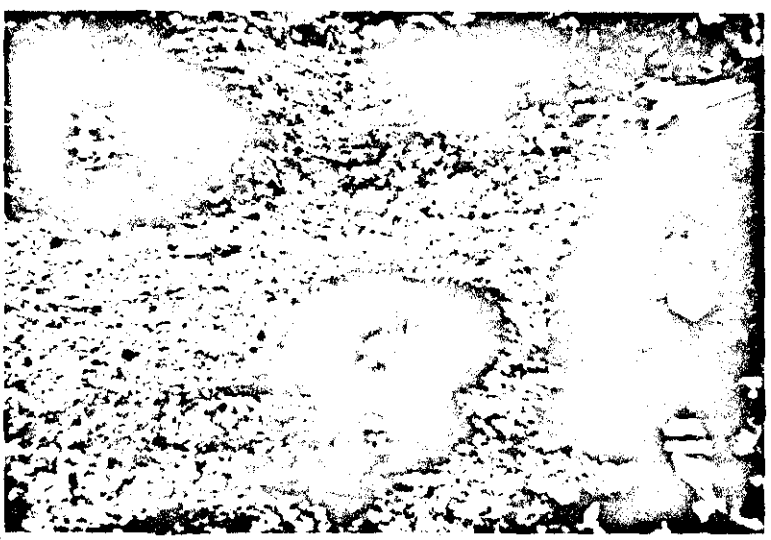

Plate 16 Photomicrograph showing chlorite alteration associated with a Stage II vein, cross nicols. Chlorite replaces sericite adjacent to vein wall (opaque on photograph). Alteration chlorite also occurs as disseminations adjacent to vein walls (opaque patches on photograph) with albite cores. Euhedral porphyroblasts in vein are albite. Dark grey matrix surrounding porphyroblasts is vein chlorite.

Chapter VI

POTASSIUM-ARGON AGE DETERMINATIONS

Although tenuous, evidence presented earlier suggests that the third period of deformation and presumably the main period of mineralization occurred between Upper Triassic (Karnian or Lower Norian) and Lower Jurassic-Upper Triassic. Because metamorphism of the chlorite-biotite gneiss of Unit 10 appears to have continued into this deformational period, three samples of gneiss were collected for potassium-argon age determinations. Samples were analysed by J.E. Harakal in the K-Ar laboratory of the Department of Geological Sciences and the Department of Geophysics at the University of B.C.

One sample of gneiss was collected south of the Baldy batholith about 5 miles east-southeast from the east end of East Barriere Lake. A second sample was collected approximately 5 miles west of the first. The third sample was collected at the headwaters of Foghorn Creek, approximately 4 miles west of the map-area. Samples selected contain little or no chlorite.

Sample Location	Material	K(%)	Ar^{40}/K^{40}	Apparent Age (m.y.)
51° 17'N, 119° 37'W	biotite	7.33 ± 0.09	0.005884	98.0 ± 3.8
51° 17'N, 119° 42½'W	biotite	7.01 ± 0.03	0.007653	126 ± 4.0
51° 31'N, 119° 56'W	Whole rock	1.19 ± 0.007	0.005998	99.8 ± 3.1

Table VII Potassium-Argon Age Determinations

The results obtained are shown in Table VII. Two samples gave ages of

98 m.y. and 99.8 m.y. These dates correspond closely to the potassium-argon dates of 98 m.y. and 103 m.y. obtained by Kirkland (1971) and 80 m.y. and 96 m.y. obtained by the Geological Survey of Canada from rocks of the Baldy batholith. It seems probable that radiogenic argon in these samples was lost at the time of emplacement of this batholith.

The third sample gave an apparent age of 126 m.y. The sample was taken approximately the same distance from the Baldy batholith as the sample which gave an apparent age of 98 m.y. and has possibly also lost some radiogenic argon during emplacement of the batholith. Although the date has probably been reset, it can be considered as a minimum age for metamorphism of the gneiss.

Chapter VII

CONCLUSIONS

The following conclusions are based on observations and discussions presented in this study:

1) Mineralization occurs almost exclusively within metasedimentary and metavolcanic rocks of the Eagle Bay Formation.
2) Copper mineralization is confined to tabular-shaped bodies which have an average east-west strike and dip fairly uniformly to the north.
3) Age of the main period of mineralization is between Upper Triassic (Karnian or Lower Noran) and Lower Jurassic-Upper Triassic.
4) Mineralization appears to post-date regional metamorphism of the host rocks.
5) The deposit appears to be genetically related to the formation of a large east-west oriented antiform located south of the map-area.
6) Large-scale structures within the antiform appear to have had an important role in the channeling of 'ore-forming' fluids.
7) 'Ore-forming' fluids are of probable hydrothermal metamorphic origin.
8) The host rocks are polydeformed and exhibit the effects of four periods of deformation.
9) The main period of mineralization appears to have been, in part, synchronous with the third period of deformation.
10) Although mineralization does not appear to be stratigraphically controlled, stratigraphy was important for the localization of higher grade mineralization.

11) Titanium-rich lithologies appear to be the best host for copper mineralization.

12) Alteration of the host rocks during the main period of mineralization involved an early recrystallization of sericite and chlorite formed by regional metamorphism and a later chloritization.

13) The contact between rocks of the Eagle Bay Formation and the chlorite-biotite gneiss (Unit 10) is an important parameter for the occurrence of 'Harper Creek-type' occurrences.

14) The contact between the gneiss (Unit 10) and rocks of the Eagle Bay Formation may represent a faulted biotite isograd.

15) Metamorphism of the gneiss continued into the third period of deformation.

16) Most sphene is of regional metamorphic origin but some occurs as hydrothermal replacements of carbonate.

REFERENCES

Badgley, P.C., 1959: Statistical Analyses of Structural Units by Steriographic and Related Projections; in Statistical Methods for the Exploration Geologist, Harper Brothers publishers, pp. 214-223.

_____, 1965: Structural and Tectonic Principles, edited by C. Croneis; New York, Harper & Row, publishers.

Campbell, R.B., 1964: Adams Lake, British Columbia; Geol. Surv. Can., map 48-1963.

Campbell, R.B. and Tipper, H.W., 1971: Bonaparte Lake map-area, British Columbia; Geol. Surv. Can., Mem. 363.

Campbell, R.B. and Okulitch, A.V., 1973: Stratigraphy and Structure of the Mount Ida Group, Vernon (82L), Adams Lake (82M W½), and Bonaparte (92P) map-areas; in Rept, of Activities, Pt. A, April to October, 1972, Geol. Surv. Can., Paper 73-1, pt. A, pp. 21-23.

Daly, R.A., 1912: Summary report on a reconnaissance of the Shuswap Lakes and vicinity, south-central, B.C.; in Geol. Surv. Can., S.R., 1911, pp. 165-174.

_____, 1914: Geology of the Selkirk and Purcell mountains at the Canadian Pacific Railway main line; in Geol. Surv. Can., S.R., 1912, pp. 156-164.

Dawson, G.M., 1895: Report on the area of Kamloops map-sheet, British Columbia; Geol. Surv. Can., Ann. Rept. 1894, vol. VII.

Dawson, G.M., 1898: Shuswap Sheet; Geol. Surv. Can., Map 604.

Ernst, W.G., 1972: CO_2-poor composition of the fluid attending Franciscan and Sambagawa low-grade metamorphism; in Geochimica et Cosmochimica Octa, 1972, Vol. 36, pp. 497-504.

Fyson, W.K., 1970: Structural relations in metamorphic rocks, Shuswap Lake area, British Columbia; in Structure of the Southern Canadian Cordilleran; Geol. Assoc. Can., Spec. Paper 6, pp. 107-122.

Hutchinson, R.W. and Hodder, R.W., 1972: Possible tectonic and metallogenic relationships between porphyry copper and massive sulphide deposits; in CIM Bull. for Feb., 1972, pp. 34-39.

Jensen, M.L., 1967: Sulfur Isotopes and Mineral Genesis; in Geochemistry of Hydrothermal Ore Deposits, edited by H.L. Barnes, New York, Holt, Rinehard & Winston, Inc., pp. 143-165.

Jones, A.G., 1959: Vernon map-area, British Columbia; Geol. Surv. Can., Mem. 296.

Kerr, P.F., 1959: Optical Minerology, third edition; New York, McGraw-Hill Book Co.

Kirkland, K.J., 1971: Sulfide Deposition at Noranda Creek, British Columbia; unpublished M.Sc. Thesis, Dept. of Geology, University of Alberta.

Meyer, C. and Hemley, J.J., 1967: Wall Rock Alteration; in Geochemistry of Hydrothermal Ore Deposits, edited by H.L. Banes, New York, Holt, Rinehard & Winston, Inc., pp. 167-232.

Nockolds, S.R., 1954: Average chemical composition of some igneous rocks; Bull. Geol. Soc. Amer., Vol. 65, pp. 1007-1032.

Osborne, W.W., 1967: Harper Creek area follow-up; unpublished report, Noranda Expl. Co. Ltd.

Poldervaart, A., 1955: Chemistry of the Earth's Crust; in Crust of the Earth--a symposium, G.S.A., S.P. 62, pp. 133-136.

Preto, V.A.G., 1970: Goof, Sue, Hail; in Geology, Exploration and Mining in B.C., B.C. Dept. of Mines & Pet. Res., pp. 297-301.

Schouten, C., 1962: Determination Tables for Ore Microscopy; published by Elsevier Publishing Co.

Schuiling, R.D. and Vink, B.W., 1967: Stability relations of some titanium-minerals (sphene, perovskite, rutile, anatase); in Geochimica et Cosmochimica Acta, Vol. 31, pp. 2399-2411.

Soregaroli, A., 1972: Harper Creek Joint Venture-Summary Report for 1971, unpublished report Noranda Expl. Co. Ltd.

Suffel, G.G., 1965: Remarks on some sulphide deposits in volcanic extrusives; in Can. Inst. Min. & Met., Trans., Vol. 68, pp. 301-307.

Uglow, W.L., 1922: Geology of the North Thompson Valley map-area; Geol. Surv. Can., S.R., 1921-A. pp. 76-106.

Walker, J.F., 1931: Clearwater River and Foghorn Creek map-area, Kamloops District, British Columbia; in Geol. Surv. Can., S.R., 1930-A, pp. 125-153.

Wanless, R.K., Stevens, R.D., Lachance, G.R. and Rimsaite, J.Y.H., 1966: Age determinations and geological studies, K-Ar Isotopic Ages, Report 6; Geol. Surv. Can., Paper 65-17, pp. 16-17.

Wanless, R.K., Stevens, R.D., Lachance, G.R. and Edmonds, C.M., 1967: Age determinations and geological studies, K-Ar Isotopic Ages, Report 7; Geol. Surv. Can., Paper 66-17, pp. 25-26.

Wanless, R.K., Stevens, R.D., Lachance, G.R. and Edmonds, C.M., 1968: Age determinations and geological studies, K-Ar Isotopic Ages, Report 8; Geol. Surv. Can., Paper 67-2, pt, A, pp. 34-35.

Westerman, C.J., 1968: Harper Creek Property, Geology; unpublished report, Noranda Expl. Co. Ltd.

Williams, H., Turner, F.J. and Gilbert, C.M., 1954: Petrography; San Francisco, W.H. Freeman & Co.

Winkler, H.G.F., 1967: Petrogenesis of metamorphic rocks, revised second edition; New York, Springer-Verlag Inc.

APPENDIX A

Description of mineral deposits within part of the
Adams Lake and Bonaparte Lake map-areas

No.[1]	Name	Location	Metals	Description	Selected References
1	Copper King (keystone Group)	51° 31'N;119° 55'W	Cu	Bands, pods and disseminations of chalcopyrite in schist	1924, p. 152[2]
2	Foghorn (Lydia)	51° 32'N;119° 55'W	Cu	Chalcopyrite as bands, pods and disseminations in schist; some chalcopyrite as fracture fillings	1916, pp. 221-222 1919, p. 179 1924, p. A152
3	Gopher	51° 32'N;119° 57'W	Cu, Pb, Zn	Mineralization reported to occur in greenschist and quartz-sericite schist	1970, p. 302
4	Shamrock	51° 32'N;119° 55'W	Pb	Quartz vein mineralized with galena	1917, p. 236 1924, p. 152 1930, p. A 145
5	Rexspar	51° 34'N;119° 54'W	U, Mo, Pb, rare earth's fluorite	Replacement body in trachyte; mineralization occurs as flat-lying lenses conformable with the enclosing schists	1949, pp. A250-A 255 1954, pp. 108-111 1957, pp. 31-32 1958, p. 30 1968, p. 164 1970, pp. 301-302

[1] for number locations refer to Figure 2.

[2] unless otherwise indicated, references refer to Annual Minister of Mines Reports, B.C. Department of Mines.

6	Smuggler	51° 34'N; 119° 54'W	Ag, Pb, Mn	Silver and lead mineralization in quartz veins	1925, p. B151 1926, p. 187 1927, p. 191 1930, pp. A192-A193
7	Minnesota Girl	51° 34'N; 119° 54'W	Ag, Pb, Zn	Mineralization occurs as fissure fillings	1924, p. 152 1926, p. 188 1930, p. 193
8	Millars Prospect	51° 35'N; 119° 54'W	Pb, Zn, Mo	Quartz veins mineralized with galena and sphalerite; minor molybdenite	G.S.C. SR 1930 A, p. 143
10	Brenda, Sonja	51° 36'N; 119° 52'W	Pb, Ag, Au, Cu		1968, p. 163
9	Bullion	51° 35'N; 119° 54'W	U	Reported trachytic volcanic rocks replaced by uraninite, pyrite and fluorite	1968, p. 164 1969, p. 229
11	Bearsden	51° 37'N; 119° 49'W	Pb, Ag, Au, Cu	Quartz vein in schist	1969, p. 228
12	Tinkirk	51° 37'N; 119° 47'W	Pb	Quartz veins mineralized with galena	1969, p. 228
13	Red Top	51° 38'N; 119° 52'W	Pb, Ag	Lead and silver minerals found in seams in a zone of shearing	1927, p. 191
14	Trophy Mt. (Summit)	51° 49'N; 119° 49'W	Pb, Zn, Ag	Sphalerite, galena with pyrite, pyrrhotite and minor chalcopyrite occur as conformable lenses in quartz-biotite gneiss	1956, pp. 69-70 1969, p. 230
15	Tim, AX, NX	51° 49'N; 119° 57'W	Mo		1968, p. 166

16	Molcop	51° 48'N; 119° 23'W	Mo, Cu	Coarse molybdenite is found in pegmatitic rocks; the pegmatites occur as pods and discontinuous veins in Shushwap gneiss; chalcopyrite with minor molybdenite also occur as disseminations in acidic dykes	1970, p. 296
17	ESP	51° 36'N; 119° 36'W	Cu	Chalcopyrite reported to occur as disseminations and conformable lenses in chlorite and quartz-sericite schists	1970, p. 296
18	Hilltop	51° 29'N; 119° 37'W	Cu	Horizon of sporadic copper mineralization in greenstone	
19	Polly Ann	51° 23'N; 119° 52'W	Mo	Molybdenite occurs in a set of widely spaced quartz veins	1964, p. 99
20	H,M	51° 22'N; 119° 51'W	Mo		1967, p. 134
21	Barriere	51° 20'N; 119° 44'W	Cu, Zn	Chalcopyrite in chlorite schists; mineralization is similar in some respects to that found at "Harper Creek"	1969, p. 233 1970, p. 314
22	Harper	51° 20'N; 119° 52'W	Cu, Pb, Zn	Reports of chalcopyrite, galena and sphalerite in schist	1962, pp. 60,61 1963, p. 59
23	Sitting Bull	51° 20'N; 119° 52'W	Cu	Quartz seams mineralized with chalcopyrite	1922, p. N146
24	White Rock	51° 18'N; 119° 53'W	Ag, Pb, Zn	Series of quartz veins and fractures mineralized with galena and tetrahedrite; some appreciable silver values reported	1927, pp. C188, C189 1928, p. 212 1950, p. A111

25	OK Group	51° 19'N; 119° 56'W	Pb, Zn, Ag	Dolomitic beds in chlorite schist; dolomites "pyritized" and contain some lead, zinc and copper minerals	1927, pp. C188, C190 1928, p. C211
26	Rainbow	51° 20'N; 119° 55'W	Pb, Zn, Ag	Descriptions of lead-zinc "replacement" bodies in schist	1927, pp. C188, C190 1928, p. C211
27		51° 20'N; 119° 54'W	Cu, Zn	Reported occurrence of chalcopyrite and sphalerite in chlorite schists	
28	Birmoly	51° 22'N; 119° 56'W	Mo	Molybdenite occurs as disseminations in an acid intrusive	1969, p. 232
29	Kuno	51° 22'N; 119° 58'W	Ag, Pb	White quartz with a pocket of high grade silver-lead ore	1927, pp. C188, C190
30	North Star (north)	51° 22'N; 119° 59'W	Pb	Limestone and quartzite with pyrite and galena	1927, pp. C190-C191 1935, pp. D7-D8 1936, pp. D36-D39
31	North Star (south)	51° 21'N; 119° 59'W	Pb, Zn, Ag Au	Quartz veins with patches of sphalerite and pyrite	1927, pp. C190-C191 1935, pp. D7-D8 1936, pp. D36-D39
32	Renning No. 1 (June)	51° 15'N; 119° 48'W	Zn, Pb, Cu	Lead-zinc-copper sulphide body in crest of small recumbent fold	1961, p. 48 1968, p. 168
33	Kajun	51° 16'N; 119° 46'W	Pb, Zn, Cu	Erratic splashes and veinlets of galena, with some chalcopyrite and sphalerite, in schist	
34	Renning, Grizzly, Cu	51° 17'N; 119° 45'W	Cu	Chalcopyrite disseminated in metasedimentary rocks	1969, p. 233

35	Bex	51° 17'N; 119° 43'W	Cu	Chalcopyrite in quartz-biotite schist	1967, p. 134 1968, p. 169 1969, p. 233
36	Silver Mineral	51° 17'N; 119° 54'W	Ag, Pb	Reports of good-grade silver-lead ore in veins	1927, pp. C188-C189 1928, p. 212
37	Rose Group	51° 08'N; 119° 41'W	Zn	Sphalerite, as fissure fillings, in limestone	1916, pp. K219-K220 1918, p. 236
38	Max, Hope	51° 08'N; 119° 47'W	Pb, Zn, Ag	Dolomitic rocks, conformable to the enclosing schists, are mineralized with galena and sphalerite	1936, p. D39 1953, p. 101 1969, p. 234
39	Homestake	51° 07'N; 119° 49'W	Ab, Ba	Barite vein with silver, tetrahedrite, galena and minor chalcopyrite; vein conformable with enclosing schists	1918, pp. 221-223 1923, pp. 147-148 1926, pp. 185, 186 1936, pp. D32-36 1964, p. 99
40	Joe, Art (Douglas and Lower Six)	51° 05'N; 119° 45'W	Pb, Zn, Ag, Cu	Outcrops of silver-lead ore occur in association with barite and in quartz veins	1930, p. A189 1966, p. 145
41	Try Me and Ranking Group	51° 05'N; 119° 45'W	Pb, Zn, Cu	Very low-grade lead-zinc-copper mineralization occurs in quartz and quartz-carbonate veins in schist	1924, p. B157 1961, pp. 53-55
42	Acacia	51° 05'N; 119° 50'W	Pb, Zn	Two seams (4in.-8in. in width) of lead and zinc sulphide lying conformably with the formation	1926, p. A186
43	New Gem and Discovery Group	51° 05'N; 119° 51'W	Pb, Zn		1926, p. A186

44	Tom, Glen (Rhode Island Lead Co.)	51° 04'N; 119° 42'W	Pb, Zn, Ag, Cu	Occurrence of lead-zinc ore in a zone of fracturing about 100' wide	1926, p. A186 1967, p. 134
45	Elmoore (Lincoln, Wallace)	51° 04'N; 119° 41'W	Pb, Ag, Zn, Cu	Breccia zone mineralized with galena, sphalerite and minor chalcopyrite	1928, p. C210 1934, pp. D28-D29 1936, p. D43 1966, p. 145
46	Lucky Coon, Elsie and White Swan	51° 04'N; 119° 38'W	Pb, Zn, Ag	Series of mineralized seams lying conformable with the schists of Shuswap series	1927, pp. C199-C200 1930, pp. A184-A185, A187 1936, pp. D39-D43
47	Speedwell, King Tut, Donnamore	51° 06'N; 119° 34'W	Zn, Pb, Ag	Bands of lead and zinc sulphide in schist	1930, pp. A185-A187 1934, p. D28 1936, pp. D40, D43
48	EX (Mosquito King)	51° 03'N; 119° 33'W	Zn, Pb	Pyrrhotite, pyrite, sphalerite and galena occur in the foliation of schists, and are further localized in minor crumples	1953, pp. A102-A103 1967, pp. 134-135
49	Mosquito King	51° 03'N; 119° 31'W	Zn, Pb, Ag	Bands of sulphide in schist	1930, pp. A186-A188 1936, p. D40
50		51° 32'N; 119° 44'W	Pb, Cu	Thin seam of galena, with minor cpy, in limestone	
51	Dunn	51° 25'N; 120° 01'W	Mo	Molybdenite in quartz veins and fractures	
52	Mike, Marge	51° 06'N; 119° 22'W	Ag, Pb, Zn	Two beds mineralized with pyrite, galena and sphalerite in sericite schist, limestone and altered limestone	1960, p. 318

53	Bet, Saul (venus)	51° 03'N; 119° 15'W	Ag, Pb, Zn	Silver-lead-zinc ore found in seams cutting limestone	1930, p. A188 1931, pp. A105-A106 1964, p. 99
54	Py Group	51° 30'N; 119° 52'W	Cu	Chalcopyrite, pyrite and pyrrhotite in schist	
55	AJS	51° 00'N; 120° 26'W	Mo, Cu	Hornblende tonalite mineralized with chalcopyrite, molybdenite and pyrite	1969, p. 234
56	PC	51° 12'N; 120° 14'W	Cu	Complex pluton mineralized with chalcopyrite	1970, p. 316
57	Allies	51° 18'N; 120° 12'W	Pb, Cu	Disseminated pyrite, galena and chalcopyrite in quartz veins	G.S.C., S.R., 1921, pp. 100A-101A
58	LK	51° 19'N; 120° 06'W	Cu	Pyrite, chalcopyrite and magnetite found in rocks of the Fennell Formation	1970, p. 313
59	Windpass	51° 27'N; 120° 05'W	Au	Gold and gold tellurides in a quartz vein which cuts a pyroxenite sill of the Fennell Formation	G.S.C., Mem. 363, p. 86
60	Hidden Creek,	51° 27'N; 120° 17'W	Cu, Ag, Au	Gold, silver and copper values reported to occur in granitic rocks of the Thuya Batholith	1968, p. 168 1970, p. 313
61	Queen Bess	51° 32'N; 120° 08'W	Ag, Pb, Zn	Veins, mineralized with galena and sphalerite, occur in greenstone of the Fennell Formation	1919, pp. K234-K236 1951, pp. 125-128
62	Jan, T.C.	51° 30'N; 120° 23'W	Cu	Mineralization reported to occur as fracture fillings in dioritic and volcanic rocks	1966, p. 143 1967, p. 132

63	RO, SO, TC, RI, LO (Friendly Lake)	51° 35'N; 120° 27'W	Cu, Mo, Ag, Pb	Disseminated argentiferous galena occurs within a shear zone; highly fractured andesite breccias contain disseminated pyrite and chalcopyrite	1968, pp. 167-168
64	Silver	51° 35'N; 120° 26'W	Cu, Zn	Skarn with pyrrhotite, pyrite, magnetite, chalcopyrite and sphalerite	1968, pp. 166-167
65	Anticlimax (Tintlhohtan Lake)	51° 35'N; 120° 18'W	Mo	Molybdenite is found in thin quartz veinlets in a small granite stock	1961, pp. 49-51 1965, p. 160 1970, pp. 304-307 G.S.C., Mem. 363, p. 85
66	Empire and Bluebird	51° 40'N; 120° 02'W	Pb, Zn	Galena and sphalerite in quartz veins in schist	1934, p. D26
67	Sonja	51° 38'N; 120° 00'W	Ag, Pb, Zn, Au, Cu		1969, p. 230
68	Polly Ann	51° 43'N; 120° 03'W	Mo	Molybdenite in a set of widely spaced quartz veinlets	1964, p. 99
69	Jud, Rex, Ax, Ab, Ti, Nx	51° 48'N; 120° 01'W	Mo	Molybdenite in Shuswap gneisses	1967, p. 131
70	Wet, Sun, Aku	51° 47'N; 120° 24'W	Mo	Quartz veins, with molybdenite, in quartz monzonite	1967, p. 131 1968, p. 166
71	CS	51° 48'N; 120° 25'W	Mo	Quartz fractures, with molybdenite, in granodiorite	1970, p. 303
72	CL, OX	51° 50'N; 120° 25'W	Mo		1968, p. 165

73	**Foghorn**	51° 32'N; 119° 57'W	Ag, Pb, Zn, Cu	Galena and sphalerite are found as fissure fillings	1913, p. 212 1915, p. 211 1916, pp. 266, 518 1917, pp. 236, 450 1924, p. 150 G.S.C., S.R., 1930 A, p. 143
74	VM	51° 31'N; 119° 42'W	Cu	Reports of chalcopyrite disseminated in schist	1970, p. 297
75	Sands Creek	51° 40'N; 120° 03'W	Mo	Molybdenite, pyrite, magnetite and scarce chalcopyrite in quartz veins and pegmatitic dykes	1961, pp. 51-53
76	Barriere East	51° 17'N; 119° 37'W	Cu	Disseminations of chalcopyrite in Gneiss	

APPENDIX B

Description of samples used For K-Ar age determinations

Barriere East Property

Sample is from recent road cut about 5 miles east southeast from the east end of East Barriere Lake. The rock contains approximately 45 percent albite, 20 percent biotite, 15 percent epidote, 10 percent quartz and minor sphene. About 1 percent of the albite, which occurs as anhedral tightly interlocking grains, is twinned. Alignment of fresh biotite imparts a good foliation to the rock. Fine-grained epidote occurs evenly disseminated.

BEX Property

Sample was taken from diamond-drill core located on the BEX property (about 5 miles west of the first sample). The rock is the same as the sample taken from the Barriere East Property.

Foghorn Property

Sample is of core collected at the headwaters of Foghorn Creek (approximately 4 miles west of the map-area). The rock contains approximately 45 percent albite, 20 percent sericite, 10 percent carbonate, 10 percent quartz, 7 percent biotite, 5 percent chlorite, 3 percent epidote, 2 percent opaques and minor sphene. Chlorite and sericite appear to occur as an alteration of biotite. Carbonate occurs in matrix and as vein fillings.

These holes stand off section on fence

SECTION I

S

N

1

2

3

5800'

5600'

5400'

5200'

5000'

4800'

4600'

4400'

Legend

Unit		Unit	
	Overburden		Graphitic and carbonaceous phyllite; minor dolomite
1	Quartzo-feldspathic phyllite; minor light green laminated greenstone	6a 6b	6a Orthoquartzite, sericite quartzite albite–sericite quartzite 6b Carbonaceous quartzite
2	Foliated, fragmental greenstone; Chlorite phyllite	8	Chlorite phyllite, quartz-chlorite-sericite phyllite, chlorite-sericite phyllite; minor chlorite quartzite
3	Chlorite phyllite	9	Altered andesite
	White to light green, well-foliated, lustrous phyllite		

scale: 1 inch equals 200 feet

2 — Diamond drill hole (arrow ace runs)

7 — Diamond drill hole (arrow ace runs)

inches

0 1 2

0 1 2 3 4 5

centimetres

BRITISH COLUMBIA GEOLOGICAL SURVEY

This reference scale bar has been added to the original image. It will scale at the same rate as the image, therefore it can be used as a reference for the original size.

8,800 E

11,200 N

11,600 N

12,000 N

12,400 N

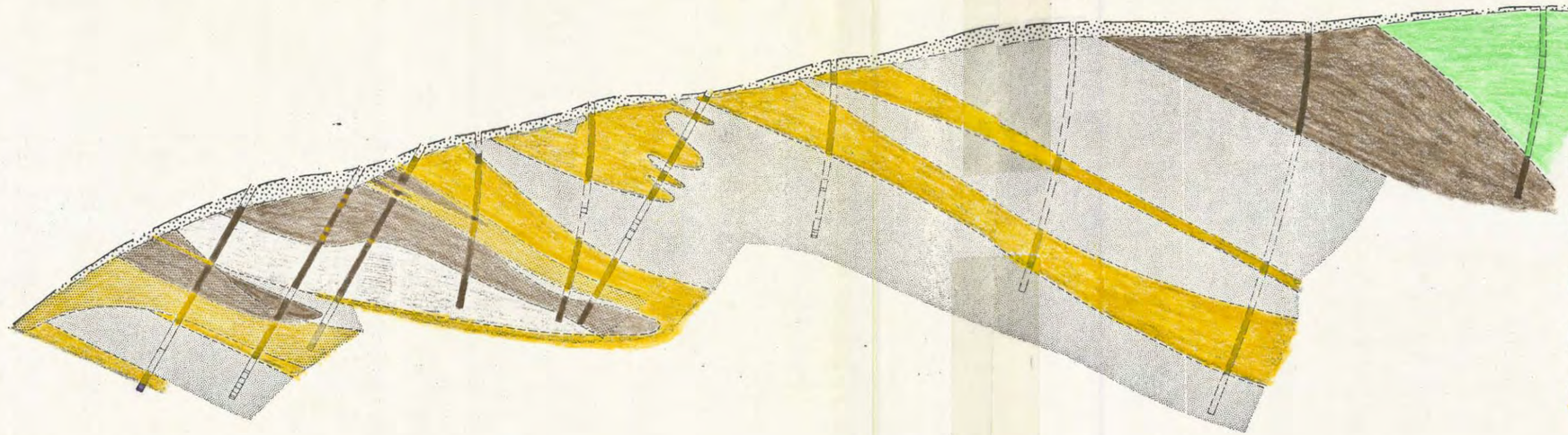

SECTION II

Legend

Unit		Unit	
	Overburden		Graphitic and carbonaceous phyllite; minor dolomite
1	Quartzo-feldspathic phyllite, minor light green laminated greenstone	6	6a Orthoquartzite, sericite quartzite albite–sericite quartzite 6b Carbonaceous quartzite
2	Foliated, fragmental greenstone; Chlorite phyllite	8	Chlorite phyllite, quartz-chlorite-sericite phyllite, chlorite-sericite phyllite; minor chlorite quartzite
3	Chlorite phyllite	9	Altered andesite
4	White to light green, well-foliated, lustrous phyllite		

scale: 1 inch equals 200 feet

2 — Diamond drill hole (with acid tests)

7 — Diamond drill hole (without acid tests)

10,000 E

inches
0 1 2
0 1 2 3 4 5
centimetres

BRITISH COLUMBIA GEOLOGICAL SURVEY

This reference scale bar has been added to the original image. It will scale at the same rate as the image, therefore it can be used as a reference for the original size.

These holes show off section on map

SECTION III

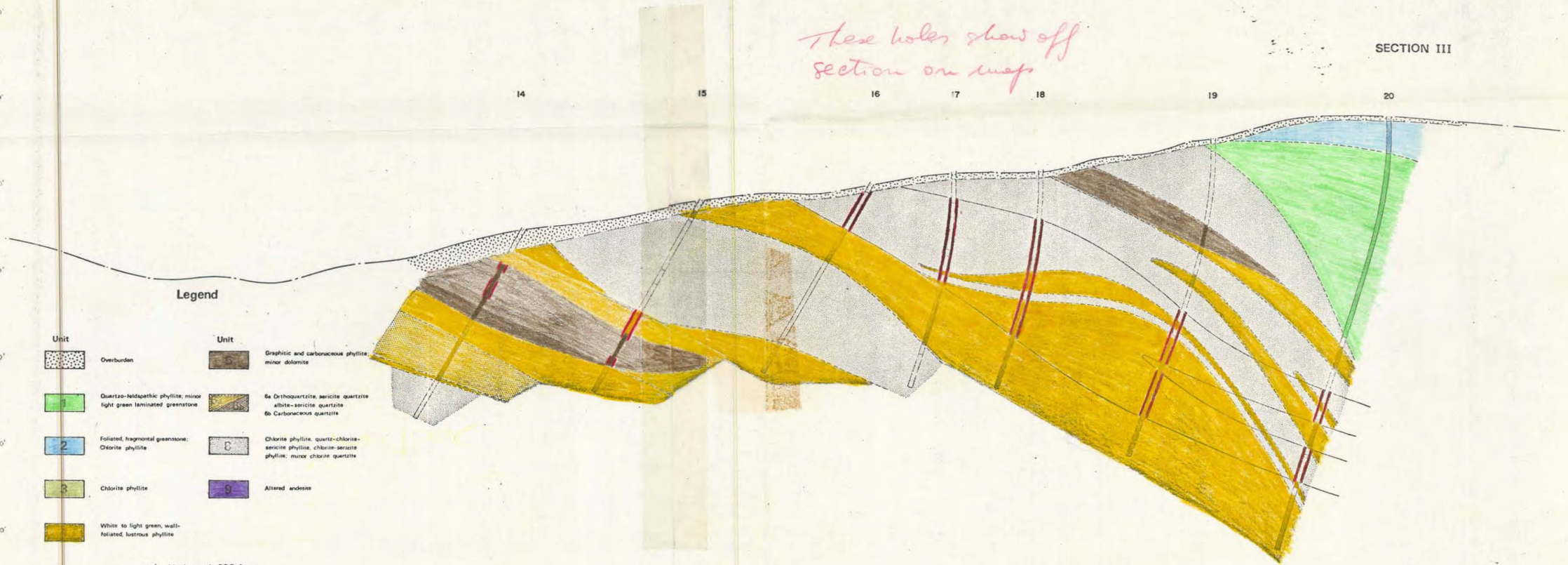

10,800 E

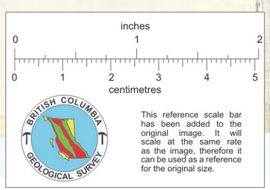

This reference scale bar has been added to the original image. It will scale at the same rate as the image, therefore it can be used as a reference for the original size.

SECTION IV

These holes show off section on map

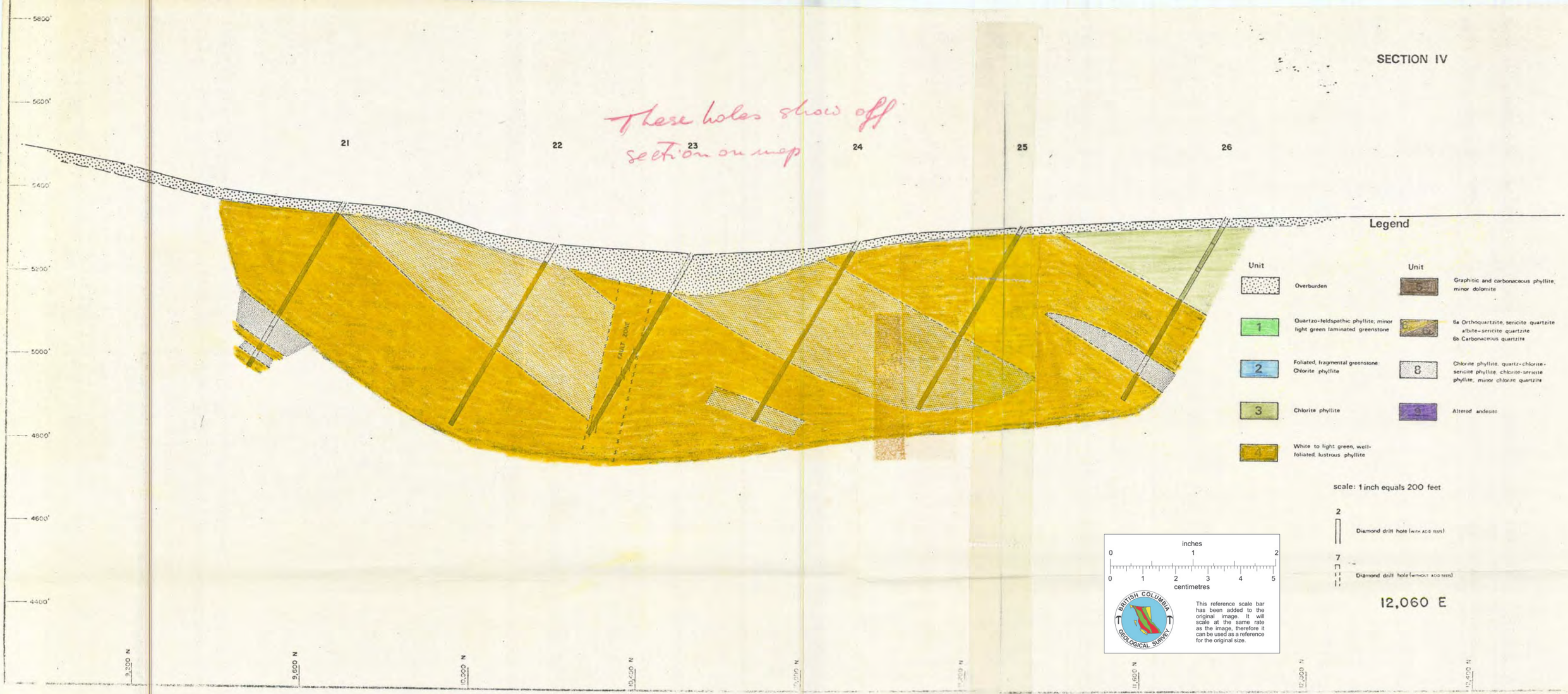

Legend

Unit		Unit	
	Overburden	5	Graphitic and carbonaceous phyllite, minor dolomite
1	Quartzo-feldspathic phyllite, minor light green laminated greenstone	6a/6b	6a Orthoquartzite, sericite quartzite albite–sericite quartzite 6b Carbonaceous quartzite
2	Foliated, fragmental greenstone: Chlorite phyllite	8	Chlorite phyllite, quartz-chlorite-sericite phyllite, chlorite-sericite phyllite; minor chlorite quartzite
3	Chlorite phyllite	9	Altered andesite
4	White to light green, well-foliated, lustrous phyllite		

scale: 1 inch equals 200 feet

2 — Diamond drill hole (WITH ACID TESTS)

7 — Diamond drill hole (WITHOUT ACID TESTS)

12,060 E

inches
0 1 2
0 1 2 3 4 5
centimetres

BRITISH COLUMBIA GEOLOGICAL SURVEY

This reference scale bar has been added to the original image. It will scale at the same rate as the image, therefore it can be used as a reference for the original size.

SECTION V

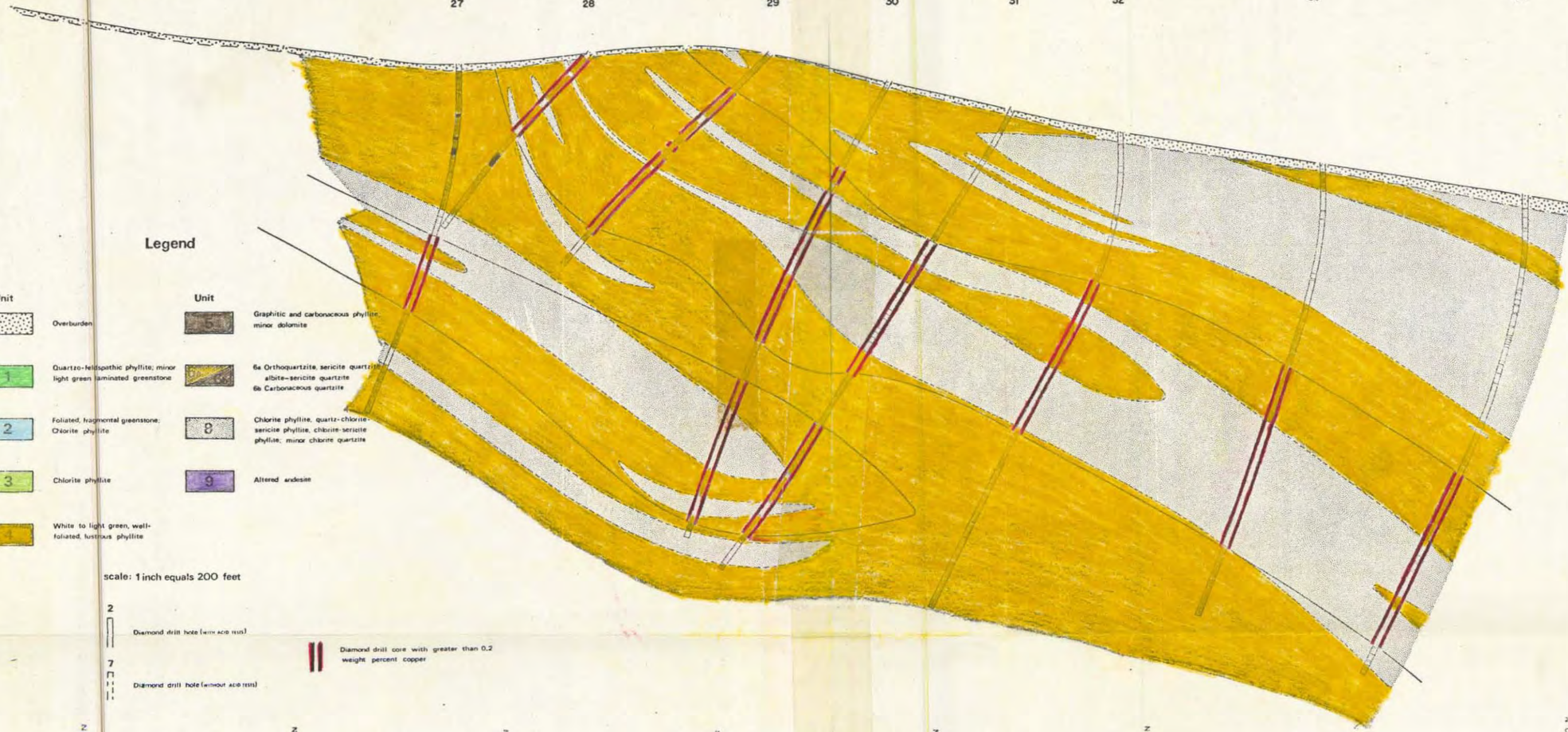

Legend

Unit		Unit	
	Overburden	5	Graphitic and carbonaceous phyllite, minor dolomite
1	Quartzo-feldspathic phyllite; minor light green laminated greenstone	6a 6b	6a Orthoquartzite, sericite quartzite, albite–sericite quartzite 6b Carbonaceous quartzite
2	Foliated, fragmental greenstone; Chlorite phyllite	8	Chlorite phyllite, quartz-chlorite-sericite phyllite, chlorite-sericite phyllite; minor chlorite quartzite
3	Chlorite phyllite	9	Altered andesite
4	White to light green, well-foliated, lustrous phyllite		

scale: 1 inch equals 200 feet

2 — Diamond drill hole (with acid tests)

7 — Diamond drill hole (without acid tests)

Diamond drill core with greater than 0.2 weight percent copper

14,200 E

inches
0 1 2
0 1 2 3 4 5
centimetres

This reference scale bar has been added to the original image. It will scale at the same rate as the image, therefore it can be used as a reference for the original size.

SECTION VI

35 36 37 38 39

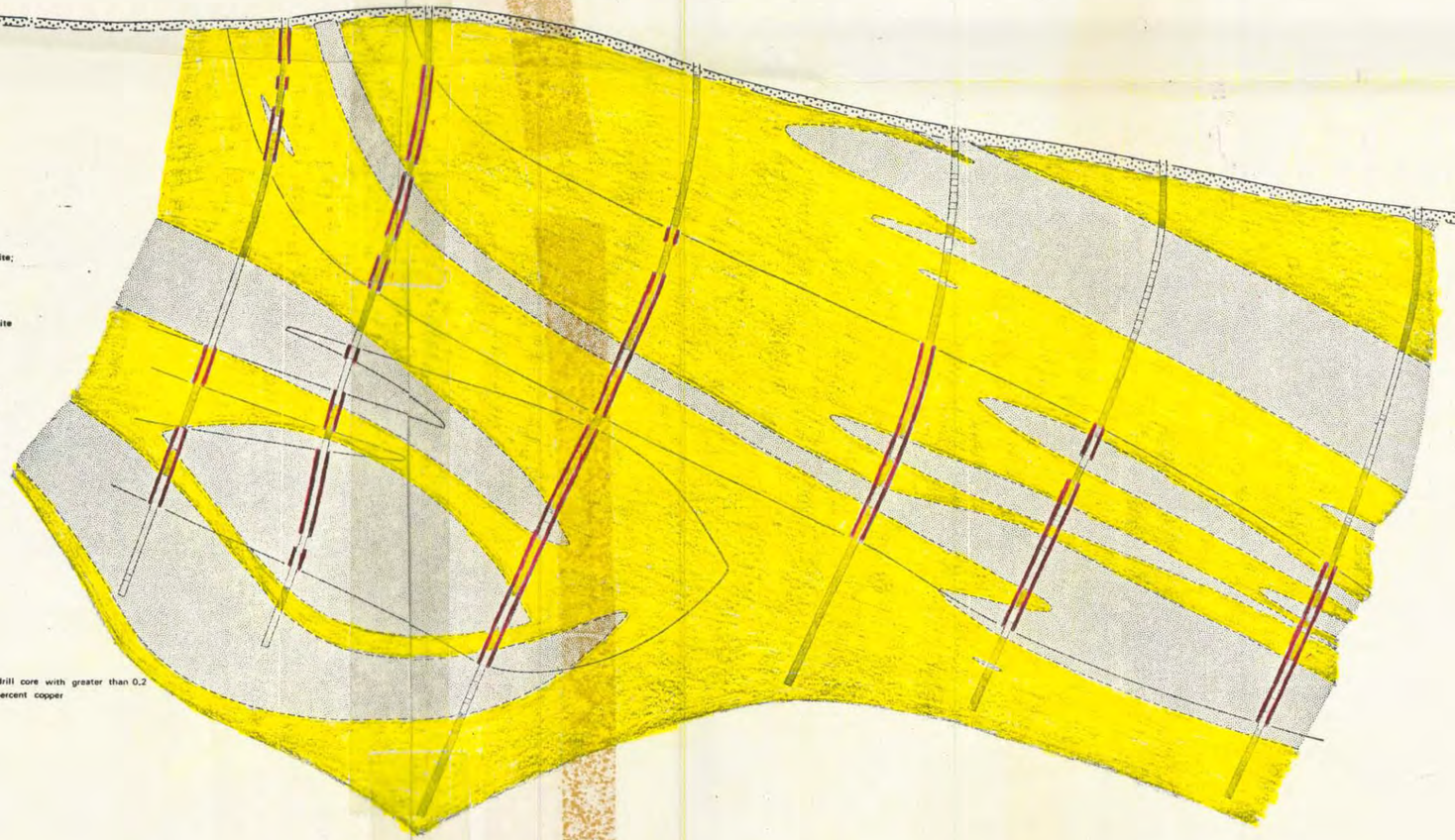

Legend

Unit		Unit	
	Overburden	5	Graphitic and carbonaceous phyllite; minor dolomite
1	Quartzo-feldspathic phyllite; minor light green laminated greenstone	6a / 6b	6a Orthoquartzite, sericite quartzite albite–sericite quartzite 6b Carbonaceous quartzite
2	Foliated, fragmental greenstone; Chlorite phyllite	8	Chlorite phyllite, quartz-chlorite-sericite phyllite, chlorite-sericite phyllite; minor chlorite quartzite
3	Chlorite phyllite	9	Altered andesite
4	White to light green, well-foliated, lustrous phyllite		

scale: 1 inch equals 200 feet

2 — Diamond drill hole (WITH ACID TESTS)

7 — Diamond drill hole (WITHOUT ACID TESTS)

Diamond drill core with greater than 0.2 weight percent copper

inches
0 1 2
0 1 2 3 4 5
centimetres

BRITISH COLUMBIA GEOLOGICAL SURVEY

This reference scale bar has been added to the original image. It will scale at the same rate as the image, therefore it can be used as a reference for the original size.

14,500 E

Fig 4. Geology map of the Harper creek copper deposit

Legend

Unit		Unit	
1	Quartzo-feldspathic phyllite; minor light green, laminated greenstone	6a 6b	6a Orthoquartzite, sericite quartzite, albite-sericite quartzite 6b Carbonaceous quartzite
2	Foliated, fragmental greestone; chlorite phyllite	7	Dark green, fragmental phyllite
3	Chlorite phyllite	8	Chlorite phyllite, quartz-chlorite-sericite phyllite, chlorite-sericite phyllite; minor chlorite quartzite
4	White to light green, well-foliated, lustrous phyllite	9	Altered andesite
5	Graphitic and carbonaceous phyllite; minor dolomite	10	Chlorite-biotite gneiss

- Schistosity
- Early fold axis
- Late fold axis (kink or open fold)
- Wrinkle lineation
- Kink fold axis plane
- Fracture (inclined)
- Fracture (vertical)
- Quartz vein
- Outcrop
- Suboutcrop
- Geologic boundary (infered)
- Fault (infered)
- Access road
- Drill hole location
- Building
- 5600 Elevation contour (in feet)
- Area with greater than 0.2 weight percent copper

Scale: ~~1 inch equals 400 feet~~

inches 0 1 2 3 4 5 centimetres

BRITISH COLUMBIA GEOLOGICAL SURVEY

This reference scale bar has been added to the original image. It will scale at the same rate as the image, therefore it can be used as a reference for the original size.

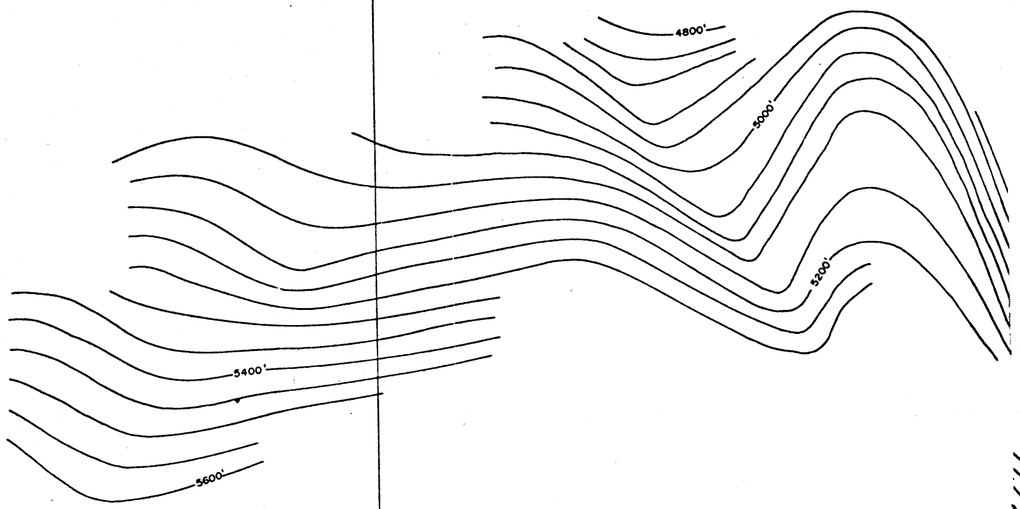

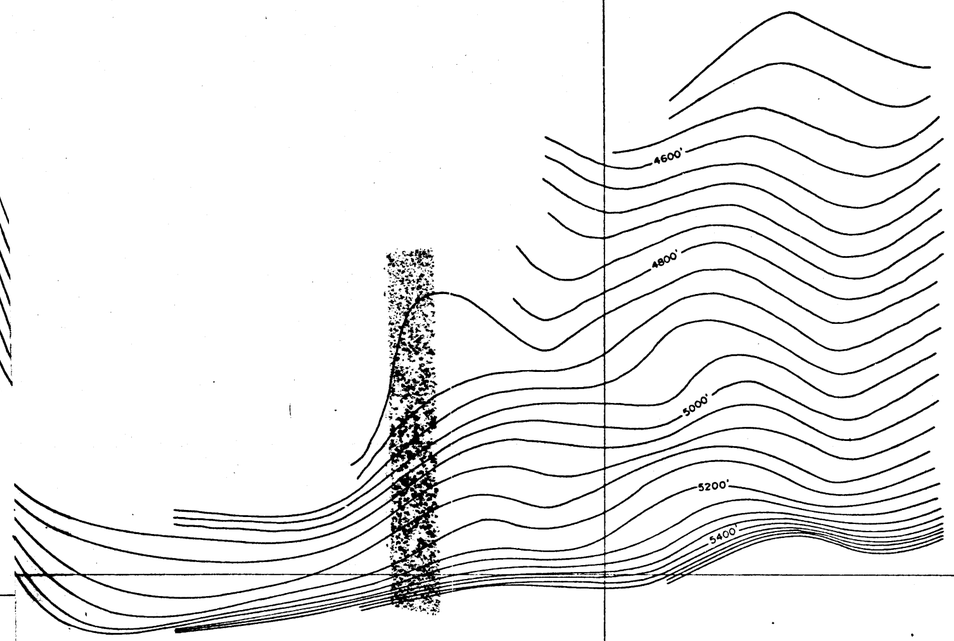

N

10,000 N

10,000 N

Fig 12. Structure Contour Map of the 'footwall' of the main copper-bearing horizon (contour interval equals 40 feet)

Scale: 1 Inch Equals 400 Feet

inches
0 1 2
0 1 2 3 4 5
centimetres

BRITISH COLUMBIA GEOLOGICAL SURVEY

This reference scale bar has been added to the original image. It will scale at the same rate as the image, therefore it can be used as a reference for the original size.